

ABSTRACT

Title of dissertation: A HYBRID MODEL FOR FATIGUE LIFE
ESTIMATION OF POLYMER MATRIX COMPOSITES

Kevin R. Uleck, Doctor of Philosophy, 2006

Dissertation directed by: Dr. Anthony J. Vizzini
Department of Aerospace Engineering

A major limitation of current fatigue life prediction methods for polymer matrix composite laminates is that they rely on empirical S-N data. In contrast to fatigue life prediction methods for metals which are based on physical crack growth models, the heart of fatigue life models for composites is empirical S-N data for each specific material system and specific loading conditions. This implies that the physical nature and processes responsible for tensile fatigue are not well understood.

In this work a mechanism-based approach is used to model the damage growth and failure of uniaxial polymer matrix composites under uni-axial tension-tension fatigue loading. The model consists of three parts: an initial damage model, a damage growth model, and a tensile failure model. The damage growth portion of the model is based on fracture mechanics at the fiber/matrix level. The tensile failure model is based on a chain of bundles failure theory originally proposed for predicting the static strength of unidirectional laminates using fiber strength distributions.

The tensile fatigue life prediction model developed in this work uses static tensile strength data and basic material properties to calculate the strength degradation due to fiber-matrix damage growth caused by fatigue loading and does not use any experimental S-N data. The output of the model is the probability of failure under tensile fatigue loading for a

specified peak load level. Experimental data is used to validate and refine the model and good correlation between the model and experimental data has been shown.

The principal contribution of this work is a hybrid-mechanistic model for analyzing and predicting the tension-tension fatigue life behavior of uniaxial polymer matrix composites. This model represents the very foundation to build upon a comprehensive model for fatigue. It demonstrates the validity of the ideas as they apply to uniaxial laminates that may in turn be used to apply to more complex laminates. Additionally, because the model is mechanism based it can be used for evaluation of the effects of constituent property changes such as matrix stiffness and toughness, or environmental conditions such as temperature and moisture.

**A HYBRID MODEL FOR FATIGUE
LIFE ESTIMATION OF POLYMER
MATRIX COMPOSITES**

by

Kevin R. Uleck

Dissertation submitted to the Faculty of the Graduate School of the
University of Maryland, College Park in partial fulfillment
of the requirements for the degree of
Doctor of Philosophy
2006

Advisory Committee:

Dr. Anthony J. Vizzini, Advisor
Professor N. Wereley, Committee Chair
Professor S.W. Lee
Professor A. Flatau
Professor H. Bruck

TABLE OF CONTENTS

Chapter 1: Introduction.....	1
1.1 Objective	1
1.2 Overview of problem	1
1.3 Limitations of Current Tools and Design Methods for Fatigue Life Analysis of PMCs	2
1.4 Scope and Contribution	3
1.5 Approach	4
Chapter 2: Literature Review	5
2.1 Mechanics of Damage and Failure in Polymer Matrix Composites	5
2.2 Failure of Unidirectional Composites	14
2.3 Fatigue Life Prediction Methods	20
2.4 Micromechanics-based Fatigue Models.....	31
2.5 Research Needs / Literature Summary	33
Chapter 3: Experimental.....	35
3.1 Objective	35
3.2 Coupon Description	35
3.3 Experimental Testing	39
Chapter 4: Theoretical Model.....	47
4.1 Overview	47
4.2 Scope and limitations	50
4.3 Physical Foundations	50
4.4 Analytical Model.....	59
4.5 Comparison of Experimental Data and Model Prediction.....	77
4.6 Parameter Sensitivity	80
4.7 Model Results.....	81
Chapter 5: Summary and Conclusions.....	86
5.1 Summary of Key Concepts.....	86
5.2 Summary of Results.....	88

5.3	Conclusions	91
5.4	Recommendations for Further Work.....	93
APPENDIX A.	References.....	94

LIST OF FIGURES

<i>Number</i>	<i>Page</i>
Figure 1: Composite fatigue damage mechanisms [reprinted from reference 34]	6
Figure 2: Talreja fatigue life diagram [51].....	8
Figure 3: Fatigue damage growth for cross ply laminates [reprinted from reference 34]....	10
Figure 4: Primary and secondary matrix cracking in a cross-ply laminate [48].....	11
Figure 5: The Critical Element concept for fatigue analysis of laminated composites (reprinted from reference 4).....	12
Figure 6: Flow chart of fatigue analysis using the critical element approach [reprinted from reference 4].....	13
Figure 7: Illustration of the principle at the core of the cumulative weakening failure model	17
Figure 8: Shear lag micromechanical model used in the Rosen cumulative weakening failure model.....	19
Figure 9: Normalized stress in the fiber and matrix near a fiber break calculated using the shear lag equations shown above using the manufacturers published mechanical properties for IM7/8552 graphite/epoxy.....	20
Figure 10: S-N plot of fatigue model W3A and Sendekyj data [reprinted from reference 44]	24
Figure 11: Predicted S-N curved for a [0/90] gr/ep laminate using stiffness degradation theory [reprinted from reference 44]	27
Figure 12: Equivalent damage curve example [12].....	28
Figure 13: Drawing and photograph of a test specimen (dimensions shown in mm).	37
Figure 14: Test specimen cure cycle data from cure on August 8, 2002.....	38
Figure 15: Test specimen Batch B tab bond cure cycle	39
Figure 16: Weibull probability density function and cumulative probability for static test data of batch B specimen tests	43
Figure 17: Load history recorded during testing (specimen H-121). The period for each cycle is 0.75 seconds. Load and stroke data was taken periodically during the testing and later examined to verify test integrity and validity.....	45
Figure 18: Fatigue test data for the 20 qualifying fatigue tests. The pink squares represent specimens that did not fail before reaching the runout criterion of 100,000 cycles.	46

Figure 19: Experimental data compared to residual strength fatigue theory given by Equation 10 (blue line) and a traditional log-linear fit. Note that these fits are purely empirical and are not based on physical damage mechanisms. Also note that the fits do not indicate a fatigue damage growth threshold.	48
Figure 20: Qualitative illustration of the idealized unidirectional composite model and typical defects found in actual composites.	53
Figure 21: A typical fiber strength distribution. The values used in the distribution shown here are for the carbon fibers from the work of McLaughlin [Reference 25].....	55
Figure 22: Cumulative distribution function and experimental data for quasi-static test specimens.	62
Figure 23: Fiber/matrix interface damage growth model.....	67
Figure 24: S-N curve calculated from Equation 32 using material properties of experimental test material.	72
Figure 25: Tensile strength probability distribution for the test material before and after fatigue cycling at $S=0.95$ for 30,000 cycles (stress given in Pa).....	74
Figure 26: Cumulative probability of failure (percent) for the test material before and after 30,000 fatigue cycles at $S=0.95$ (ordinate axis units are Pa)	75
Figure 27: Example of the cumulative probability of fatigue failure predicted by the analytical model using the mechanical properties of the test material	77
Figure 28: Experimental data distribution compared to predicted fatigue life distribution .	79
Figure 29: Effect of Strain Energy Release Rate Change on the predicted fatigue life distribution for $S=0.95$	81
Figure 30: Static strength distribution for the test material showing damage growth threshold and peak applied stress for $S=0.95$	84
Figure 31: Functional summary of the fatigue life model developed in this work.....	90

ACKNOWLEDGMENTS

The author wishes to thank his academic Advisor, Dr. Anthony J. Vizzini, who has shown unwavering support throughout the author's collegiate experience. Additionally, the author would like to acknowledge the Composites Research Laboratory at the University of Maryland which supported this work.

Finally, the author wishes to extend his deepest gratitude to his wife, family, and friends for their support and patience.

CHAPTER 1: INTRODUCTION

1.1 Objective

The overall objective of the work described in this dissertation is the development and demonstration of a mechanism-based model for the fatigue life of unidirectional polymer matrix composites. This model is based on physical damage mechanisms at the fiber/matrix scale and its formulation does not rely upon empirical S-N data. The intent of this work is to contribute to the fundamental understanding of the fatigue effect in polymer matrix composites by demonstrating through an analytical fatigue life model that the fundamental damage mechanism that are responsible for fatigue in uniaxial polymer matrix composites is *fiber/matrix interface damage*.

1.2 Overview of problem

To enable increased use of advanced polymer matrix composites in primary structure applications, questions regarding the reliability and lifetime performance of the materials must be answered. Several recent high-profile failures of composite structures have highlighted the unknowns associated with the use of composites. A prime example is the failure of the vertical stabilizer on an Airbus A-310 airliner that occurred in 2001. In light of that and other incidents questions pertaining to the reliability of composites structures and the wide variation of analysis methods used to design and evaluate them have highlighted the lack of fundamental understanding of composite damage and failure mechanisms.

As previously stated, the objective of this work is to further the fundamental understanding of damage growth and failure of polymer matrix composites under tensile fatigue loading conditions. In the Literature Review section examples of methods for describing damage growth and failure for PMCs under tensile fatigue loading are presented. Close examination of these methods and models reveals that the fundamental physical mechanisms responsible for fatigue of composite materials are not represented and furthermore, are not fully understood. In particular, there is no complete mechanistic model for damage growth in and failure of uniaxial laminates or plies. This is a critical component of general composite fatigue theory because the failure of a general laminate is dependent on the failure of the primary load carrying plies within it (as described in section 2.1.4, *Critical Element Theory*). The theory described in this dissertation is a major step toward addressing that critical missing part.

1.3 Limitations of Current Tools and Design Methods for Fatigue Life Analysis of PMCs

Current fatigue life and reliability analysis methods for polymer matrix composite laminates are almost exclusively based on empirical *rules* developed for particular material systems and applications. Although various levels of physical mechanical analysis are often used in the development of these methods, close inspection reveals that almost all of them fundamentally rely on *curve fits* of experimental data. As a result, the fundamental damage mechanisms and the role of material properties that are responsible for failure are

not directly addressed. This amounts to a major limitation of the current fatigue life analysis tools because they must be calibrated to each specific set of material properties and loading conditions. Examples of the current fatigue life analysis methods are given later in the Literature Review section of this dissertation.

1.4 Scope and Contribution

The theory described in this dissertation focuses on damage growth and failure of unidirectional composite laminates under axial tension-tension fatigue loading. It is applicable to continuous fiber, polymer matrix laminates such as those used in high performance aircraft structures. Understanding and modeling of the fatigue behavior of unidirectional laminates is critical to understanding fatigue failure of more general composite laminates because the fatigue life of a uniaxial laminate is the limiting factor for the tension-tension fatigue life of a general, angle-ply laminate (see section 2.1.4).

The principal contribution of this work is a hybrid-mechanistic model for analyzing and predicting the tension-tension fatigue life behavior of uniaxial polymer matrix composites. This model is not based on S-N data; instead basic material properties (such as stiffness) and quasi-static strength test data are used to predict damage growth and failure as a result of fatigue loading. The output of the model is a residual tensile strength or failure distribution and therefore differs from the deterministic S-N curve type of analyses that are commonly seen. This model represents the very foundation to build upon a comprehensive

model for fatigue. It demonstrates the validity of the ideas as they apply to uniaxial laminates that may in turn be used to apply to more complex laminates.

1.5 Approach

The theory developed in this work has roots in two major areas: fracture mechanics and non-deterministic methods. Fracture mechanics techniques are employed to model damage growth between the fibers and matrix, and non-deterministic analysis methods are used to characterize the initial damage state and the probability of failure as a result of fatigue loading. The two methods complement each other in the approach taken for this work. By applying non-deterministic methods, fracture mechanics methods applied at the micro-mechanical level can be used to describe the macro-mechanical behavior of a composite laminate. In other words, the use of non-deterministic methods allows fracture mechanics techniques to be applied to the composite material as if it were a homogenous, single-phase material with *smearred* properties in a way analogous to the classical mechanical analysis methods for composites.

CHAPTER 2: LITERATURE REVIEW

To begin this discussion on fatigue of composite materials, it is beneficial to highlight several important differences between composite materials and metals with respect to damage and fatigue behavior. In the most general sense, material fatigue is caused by any non-conservative deformation process in which energy is lost as a result of the creation of new surface area. In metals, the initiation and growth of a single dominant crack governs the fatigue life of the structure. In contrast, fatigue of laminated composites materials, which are inherently anisotropic and multiphase, is due to multiple damage mechanisms with growth both parallel and perpendicular to the applied loading, none of which consistently dominates. Furthermore, damage growth in composites depends on many factors including direction of applied load, layup, ply stacking sequence, relative stiffness of the fiber and matrix, and loading rate. [35]

The theory developed in this dissertation uses ideas and concepts from several different areas such as micro-mechanics, fracture mechanics, and non-deterministic analysis. As such, this Literature Review is separated into several sections each focusing on distinct concept areas.

2.1 Mechanics of Damage and Failure in Polymer Matrix Composites

This section discusses the qualitative physical aspects of damage and failure for tension-tension fatigue of fiber reinforced polymer matrix composites.

2.1.1 Damage Mechanisms in Unidirectional Polymer Matrix Composites

Because the subject of this dissertation is fatigue of uniaxial continuous-fiber reinforced composites, it is first necessary to examine and understand the damage mechanisms and failure mechanics that develop under uniaxial tensile loading. Damage in polymer matrix composites can take a variety of forms and the different damage mechanisms often interact with each other. For the scope of this work, the mechanisms of interest are the in-plane modes that develop under uniaxial tensile loading.

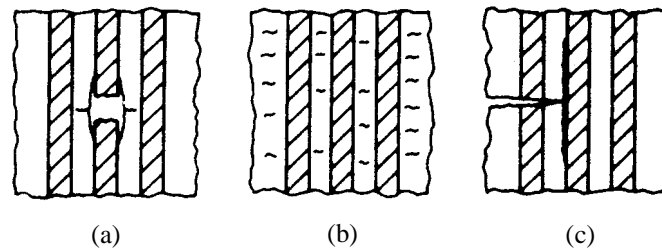


Figure 1: Composite fatigue damage mechanisms [reprinted from reference 34]

There are three fundamental damage mechanisms that occur in uniaxial tensile loaded composites: fiber fracture, matrix cracking, and fiber/matrix interface failure [34]. Other forms of damage that are sometimes discussed, such as fiber pull-out and fiber bridging, are combinations of these three fundamental mechanisms.

Fiber fracture (Figure 1a) occurs when the applied stress on the fibers is greater than the lower bound of the fiber strength distribution. When a fiber breaks, shear stress concentrations can lead to matrix cracking and debonding at the break. Matrix cracking

(Figure 1b) occurs when the applied cyclic strain is greater than the matrix fatigue limit. Transverse microcracks often initiate between fibers and then grow until they reach a fiber boundary. There they may stop or cause a local stress concentration sufficient to cause the fiber to fail. Finally, the fiber/matrix interface may undergo shear failure (Figure 1c).

Although these basic damage mechanisms are distinct, they interact and are interdependent. Of specific interest is fiber-matrix interface damage (or failure). It has been observed that for stiff-fiber reinforced composites, the fiber-matrix interface is inevitably damaged as a result of local fiber or matrix failures.

2.1.2 Fatigue Damage Mechanisms in Unidirectional Composite Laminate

Dharan [9] has observed that for unidirectional laminates, each of these mechanisms is dominant over a particular range of cyclic loading. In the case of highly loaded, short fatigue life ($N < 10^2$) tests, fiber breakage is the dominant mechanism. Lorenzo and Hahn [22] have shown that this fiber breakage leads to transverse matrix cracking and fiber/matrix interface failure. On the first load cycle, the weaker fibers break causing local stress concentrations. Upon successive loading, these local stress distributions cause neighboring fibers to fail thereby nucleating damage. Soon local damage sites grow together and the laminate fails.

For moderately loaded, medium life fatigue tests ($10^2 < N < 10^6$), matrix microcracking is the dominant mechanism. Transverse matrix microcracks form and propagate through cyclic loading until reaching a fiber interfaces. At the interface the crack may simply stop,

promote fiber/matrix interface failure, or cause the fiber to fail. After substantial cycles, the sum of the damage caused by matrix microcracking causes the laminate to fail.

Under light cyclic loading, where the applied strain is below the matrix fatigue limit, it has been experimentally observed that no substantial damage develops and the laminate has an indefinite fatigue life.

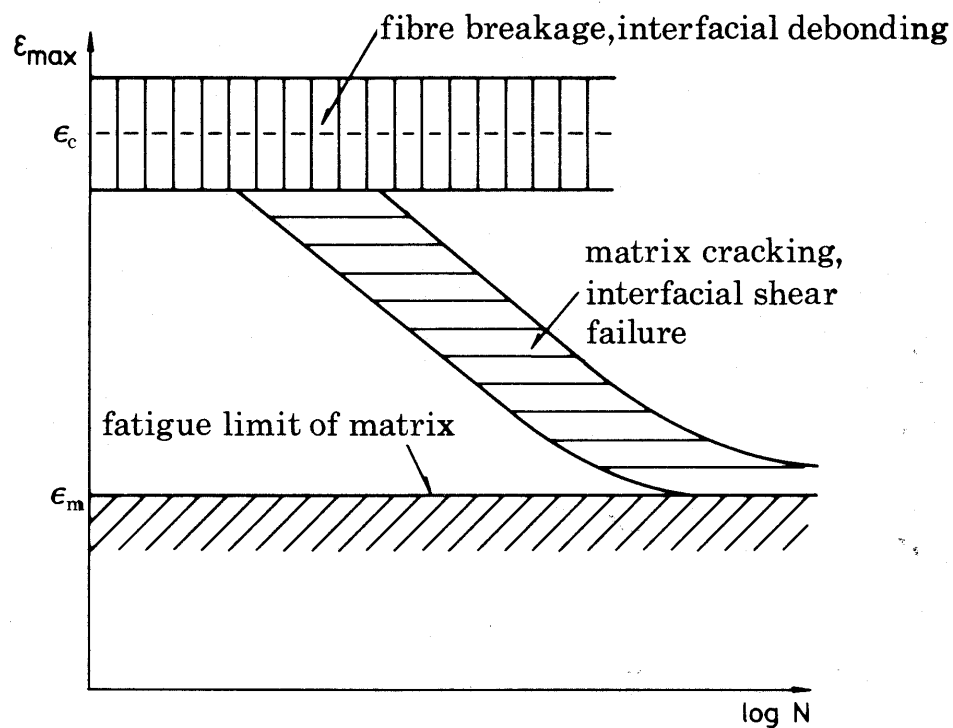


Figure 2: Talreja fatigue life diagram [51]

Combining these observations, Talreja [51] developed a fatigue life diagram for unidirectional composites (Figure 2). The high stress region is bounded by the unidirectional laminate failure scatter band, and represents low cycle fatigue behavior where fiber breakage is the dominant mechanism. Next, the sloping band represents the

effect of matrix microcracking and interface failure on the fatigue life of the laminate. Finally, the lower bound is the fatigue limit of the matrix, below which no failure will occur. Note that the only the sloping middle band represents progressive damage. It is assumed that at high load levels, damage is *not* progressive but instead a process of random fiber failures.

Additionally, note that the strain is used as the load parameter instead of stress. At a given strain state, the fiber and matrix will both be at the same strain level but the stress in each will be very different due to the difference in modulus. For this reason, Talreja suggests that strain is a more appropriate parameter for describing damage development in composite materials.

2.1.3 Fatigue Damage in Cross-Ply Composite Laminate

Fatigue damage in cross-ply laminates is due to the same mechanisms as in unidirectional laminates, however the progression and type of damage differs. Reifsnider [34] has developed a general damage progression model for cross-ply laminated composites that has been widely accepted. This model divides the damage progression curve for a given material into three stages: early life, mid-life, and final failure. Figure 3 is a graphical representation of this model.

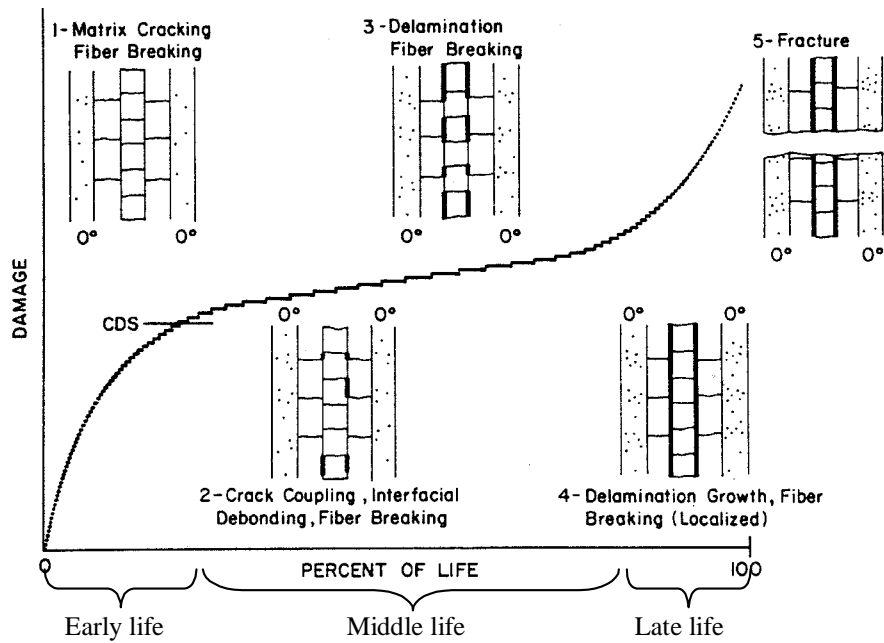


Figure 3: Fatigue damage growth for cross ply laminates [reprinted from reference 34]

During the first phase of damage development in a fatigue test, matrix cracks perpendicular to the load direction form in the off axis plies. These are called *primary cracks*. The crack density (size, spacing, and quantity) soon reaches a saturation point that Reifsnider has called the Characteristic Damage State, or CDS.[48] It has been observed that the CDS is a laminate property.

Once the laminate has been damaged to its CDS, it enters the second phase of damage development. Here damage grows at a significantly slower rate than during the first phase. The primary damage event during phase two is the formation of secondary cracks parallel to the ply. Additionally, fiber fractures are caused by stress concentrations at the intersection of primary and secondary matrix cracks.

In the final stage of fatigue life, delamination initiates at the intersection of primary and secondary cracks and quickly propagates (see Figure 4). The result of this delamination is that the composite no longer behaves as a single laminate, and load sharing between the plies is greatly reduced.

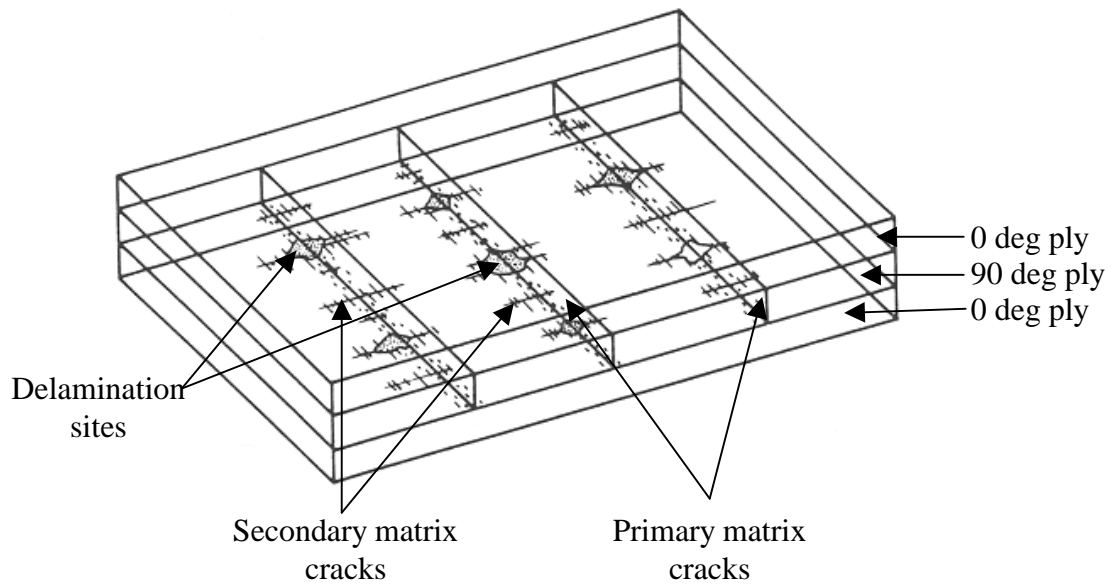


Figure 4: Primary and secondary matrix cracking in a cross-ply laminate [48]

2.1.4 Critical Element Theory

The “critical element” concept was first formalized by Reifsnider and Stinchcomb in 1986 [36] and has become a widely accepted conceptual framework for modeling and analyzing the fatigue behavior of laminated composites. The essentials of the critical element model are shown schematically in Figure 5. Such an approach is based upon the assumption that the damage associated with property degradation is widely distributed within the composite laminate. In addition, it is assumed that a representative volume can be chosen such that the

state of stress in that volume is typical of all other volumes in the laminate, and that the details of stress distribution and damage accumulation in that volume are sufficient to describe the final failure resulting from a specific failure mode. Thus, it is possible to select different representative volume elements for different failure modes. We proceed by further dividing the representative volume into “critical” and “sub-critical” elements. The critical elements are selected in such a manner that their failure controls the failure of the representative volume and therefore (by definition of the representative volume) of the laminated component. The remainder of the elements in the representative volume are regarded as sub-critical because their failure does not cause failure of the representative volume and, therefore, of the component. Their failure (due to such events as cracking or delamination) does, however, lead to greater stresses in the critical element that contribute to the eventual failure of the component.

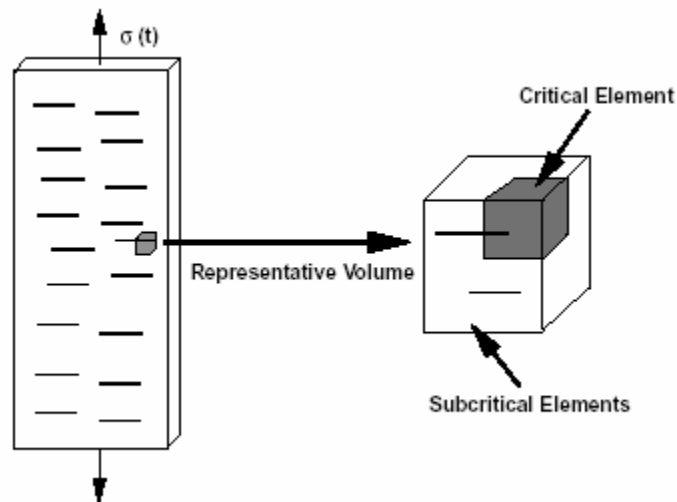


Figure 5: The Critical Element concept for fatigue analysis of laminated composites (reprinted from reference 4)

As an example of such a failure process, the case of tensile fatigue failure of a cross-ply laminate shall be considered. During the fatigue process, matrix cracks develop in the 90° plies. However, these cracks do not cause failure of the laminate. They do increase the stress level in the 0° plies. But it is only when the 0° plies fail that the laminate fails. Thus, in this simple example, the 0° plies correspond to the critical element and the 90° plies correspond to the sub-critical element. The calculation of remaining strength and fatigue life is then carried out within the critical element as shown in Figure 6.

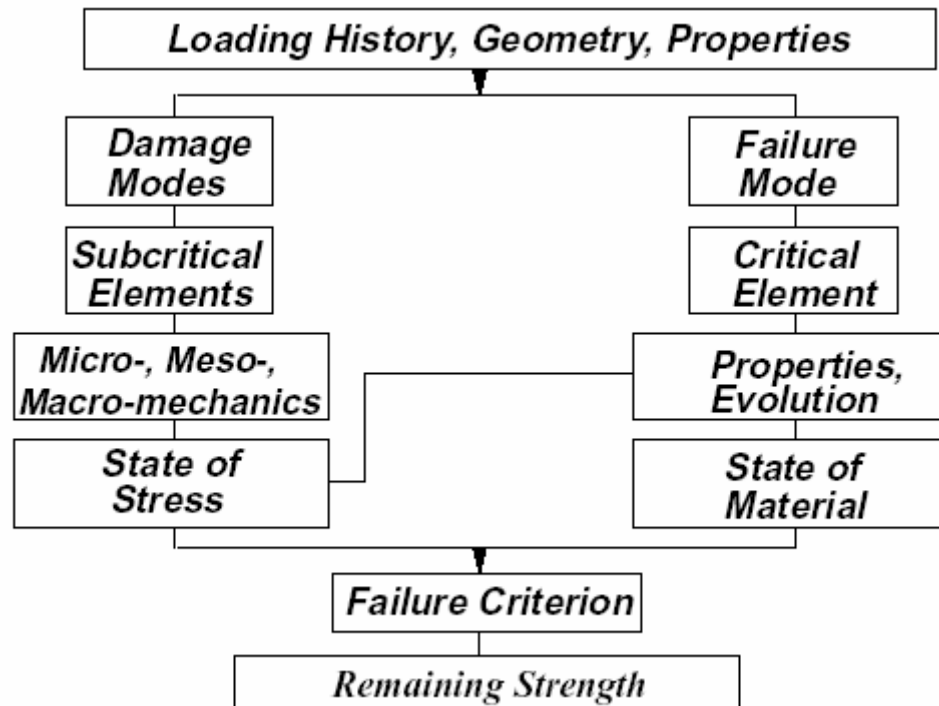


Figure 6: Flow chart of fatigue analysis using the critical element approach [reprinted from reference 4]

Note that as a direct consequence of the assumption that the critical element controls fatigue of the laminate, the fatigue life of the critical element also provides an upper bound

for the laminate fatigue life. Furthermore, the prediction for the fatigue life of the critical element forms the foundation for the prediction of the fatigue life for the whole laminate.

2.1.5 *Summary of Fatigue Damage Mechanics in Polymer Matrix Composites*

Several important conclusions relevant to this work can be drawn from the literature. They are as follows.

- For general angle-ply laminates, the *critical element* controls the fatigue life. The other plies in the laminate affect the stress state of the critical element but do not directly drive fatigue failure.
- Several different damage modes occur in tension-tension fatigue of composites. For unidirectional plies under axial loading they are: fiber fracture, matrix micro-cracking, and fiber-matrix interface failure..

2.2 **Failure of Unidirectional Composites**

In section 2.1.4 it was shown that the behavior of the unidirectional ply is the governing factor for tension-tension fatigue of continuous fiber composite materials. Therefore, accurate understanding and analysis of the fatigue process in unidirectional composites is fundamental to understanding the fatigue response for more general composite laminates.

Fatigue damage refers to the degradation of structural integrity as a result of cyclic loading. The goal of fatigue analysis is to predict this degradation and thereby predict the occurrence of structural failure. Structural failure itself can have different definitions,

being broadly defined as the inability of a structure to perform within a given threshold. For the case of fatigue loading, catastrophic failure or the complete loss of load carrying ability is often the point of interest. As a first step to understanding the tension-tension fatigue failure of uniaxial composites, it is useful to examine several of the analysis methods for uniaxial composites to establish a foundation on which a progressive/fatigue failure model can be developed.

2.2.1 Fracture in Continuous Fiber Composites

Analytical models for prediction of the static tensile strength of unidirectional composites form the heart of composite structural mechanics. A variety of models and methods exist, yet none have been widely embraced or accepted by the composite structures community. [2,46] For practical reasons, most composite analysis methods in use today treat the unidirectional ply as a homogenous anisotropic material with a single strength value for the axial direction. The result of this treatment is that fracture-based failure mechanisms are largely ignored and consequently composites are analyzed using strength-of-materials like methods. This is acceptable for many structural analysis cases, but not for all, especially for the case of cyclic or fatigue loading.

2.2.2 Cumulative Weakening Tensile Failure Theories

One important class of micromechanics based tensile failure theories are known as *cumulative weakening* or *chain-of-bundles* theories. [3,10,16,32,37,45] These theories characterize the tensile strength of unidirectional composites using the load transfer

characteristics of the fiber/matrix interface. The key idea in these theories is that the length required to transfer axial load between the fiber and the matrix is a primary driver of the tensile strength of a uniaxial composite. A broken or otherwise discontinuous fiber carries a reduced load in the vicinity of a break due to shear lag. Over this distance (where the fiber stress is less than the nominal fiber stress) the fiber can be considered ineffective and the load deficit must be supported by the neighboring intact fibers. The composite can therefore be modeled as a chain of links whose length is characterized by the length required for shear lag transfer of load from the fiber to the matrix. When too many ineffective fibers accumulate within a link length, the remaining intact fibers become overloaded which leads to catastrophic tensile failure of the entire composite.

The Cumulative Weakening Failure theory was first developed by Rosen [37] in 1964. Rosen postulated that for axial failure of a unidirectional ply to occur a sufficient number of fiber fractures must accumulate within a critical length, δ , which is equal to the length required for a broken fiber to be fully loaded via shear lag through the matrix. For lengths less than δ , there is insufficient length for the fiber to be loaded to the nominal load level through shear loading and the load deficit is then taken up by adjacent fibers. If many fiber fractures occur within the critical length, the remaining unfractured fibers will be overloaded and the ply will fail. Figure 7 illustrates this theory. In the top and bottom sections of length δ , a few individual fibers have fractured but the remaining fibers are able to carry the load difference without failing. In the center section however, many fibers have failed so the remaining unbroken fibers are overloaded causing them to fail.

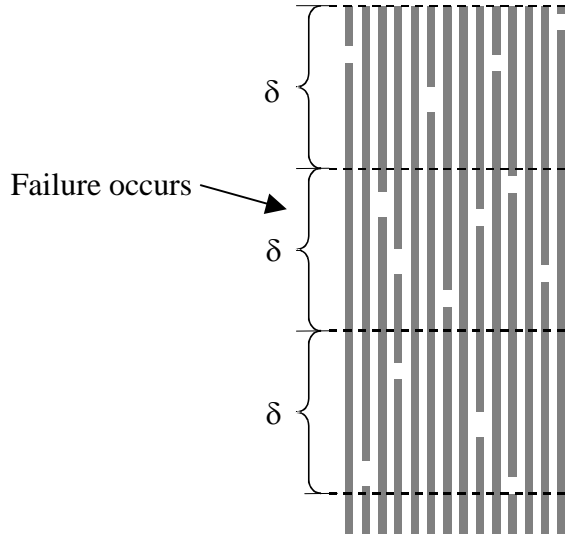


Figure 7: Illustration of the principle at the core of the cumulative weakening failure model

Using a basic shear lag model (defined below), the axial distance from a fiber break required for a fiber to achieve a fraction ϕ of the nominal fiber stress is given in Equation 1. This is known as the fiber link length or the fiber ineffective length.

$$\delta_e = \frac{d_f}{2} \left(\frac{1 - \sqrt{v_f} E_f}{\sqrt{v_f} G_m} \right) \cosh^{-1} \left(\frac{1 + (1 - \phi)^2}{2(1 - \phi)} \right)$$

Equation 1

The most probable static tensile strength of a unidirectional composite laminate can then be determined by using the fiber link length (δ) and the fiber bundle strength Weibull distribution parameters (α, β) as shown in Equation 2. [37]

$$\sigma_{ULT} = (\alpha \delta \beta e)^{-1/\beta}$$

Equation 2

2.2.2.1 Micromechanical Model for Chain-of-Bundles Theories

The micromechanical shear lag model which Rosen used for determination of the fiber ineffective length (Equation 1) is shown in Figure 8. Note that this is *not* the same as a basic single-fiber model because the discontinuous fiber is surrounded by an elastic bulk material instead of a rigid boundary. The key assumptions and definitions used in this model are as follows:

- The fiber is assumed to have a circular cross section with diameter d_f and elastic modulus E_f .
- The strain in *Bulk Material* is constant and equal to the nominal far-field composite strain.
- At the fiber break location ($\zeta=0$), the axial stress in the fiber is zero ($\sigma_{11}=0$).
- The matrix is perfectly bonded to the fiber and behaves in a perfectly elastic manner having a shear modulus G_m up to its ultimate shear strength, γ_{ULT} .
- Tensile forces in the matrix are small and can be neglected.

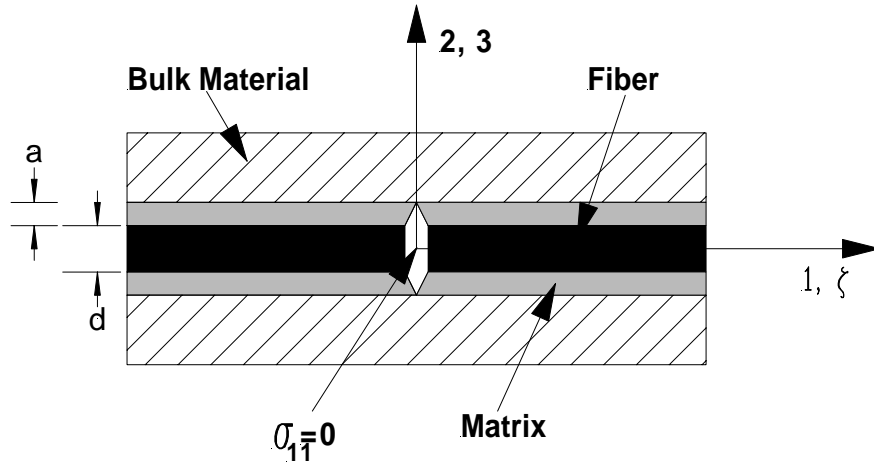


Figure 8: Shear lag micromechanical model used in the Rosen cumulative weakening failure model

Using this model, the following equation for the shear strain between the fiber and the matrix can be derived:

$$\gamma = \frac{\sigma_{f_0}}{2G_M} \left(\frac{G_M}{E_f} \right)^{1/2} \left(\frac{\sqrt{v_f}}{1 - \sqrt{v_f}} \right)^{1/2} (\cosh \eta \zeta - \sinh \eta \zeta)$$

Equation 3

where:

$$\eta^2 = \left(\frac{G_M}{E_f} \right) \left(\frac{\sqrt{v_f}}{1 - \sqrt{v_f}} \right) \left(\frac{2}{d_f} \right)^2$$

Equation 4

The stress in the fiber near the break is then given by:

$$\sigma_f = \sigma_{f_0} (1 + \sinh \eta \zeta - \cosh \eta \zeta)$$

Equation 5

Normalized stresses calculated using equations 3 and 5 as a function of distance from the fiber break (ζ) are plotted below in Figure 9. The material properties used in this plot are those of the material used in the experimental testing as described in section 3.2.1.

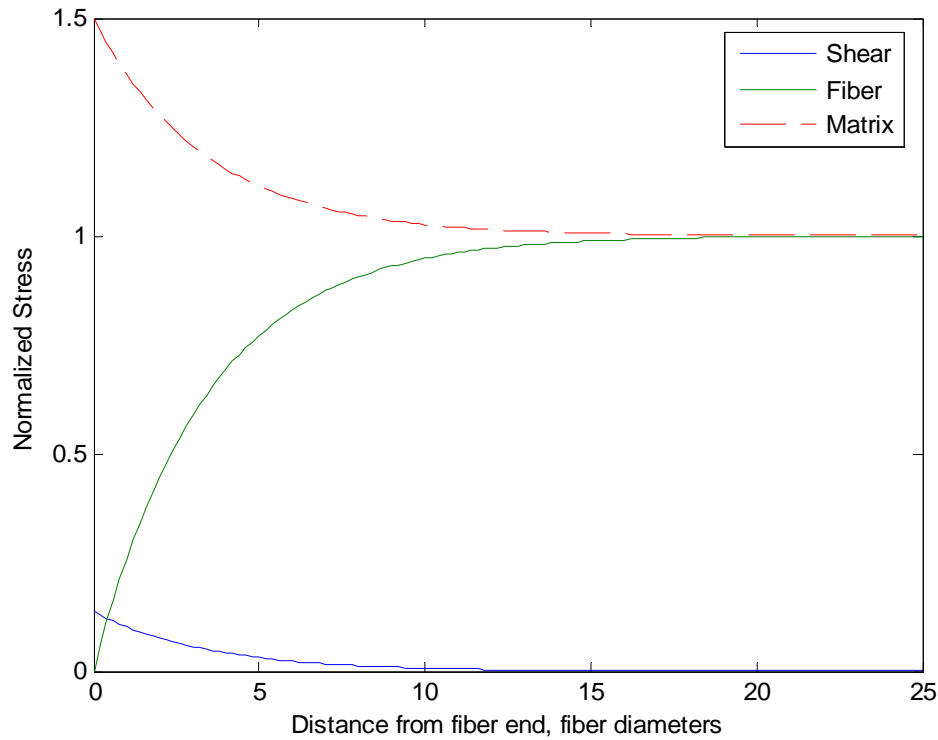


Figure 9: Normalized stress in the fiber and matrix near a fiber break calculated using the shear lag equations shown above using the manufacturers published mechanical properties for IM7/8552 graphite/epoxy.

2.3 Fatigue Life Prediction Methods

Fatigue life prediction theories fall into five categories ranging from completely empirical to analytical. An important variation between the theories is the choice of damage metric, or the physical property used to quantify damage. Traditionally, three damage metrics have been used: residual strength, residual stiffness, and to some extent, matrix crack density.

2.3.1 Empirical Fatigue Theories

The basis of empirical fatigue theories is simply modeling the S-N curve of a particular laminate, i.e. forming a curve fit. These are useful when knowledge of the damage mechanisms is lacking or the damage process is too complicated to model and sufficient data exist to allow for interpolation within the results. Consequently, the first fatigue theories for composite materials were of this type. Many theories have been formed beginning with a simple power law (similar to the Paris law used for metal fatigue) to more complex models that attempt to incorporate additional variables or constants. Several examples as given by Sendekyj [44] are included as Equation 6 through Equation 8.

$$\frac{\sigma_{ult}}{\sigma_a} = N^S$$

Equation 6

$$\sigma_a = \sigma_{ult} - b \log N$$

Equation 7

$$\sigma_{range} = a + b / N^x - c / A^y$$

Equation 8

Where:

σ_a : maximum applied stress

σ_{range} : stress range

x, y, b, c, S : material constants

$$A = (1 - R)/(1 + R) = \sigma_{range} / \sigma_{mean}$$

A common shortcoming of these theories is that they provide no insight into the physical mechanisms responsible for damage development. This is illustrated in Equation 6 through Equation 8 by observing that they do not contain a damage metric. As such, they are not predictive and therefore require a large database for each material, stacking sequence, and testing condition.

Another more critical problem is that these curve fits are limited to uniaxial, constant amplitude cyclic loading. To deal with this, various authors have proposed methods to extend these theories to multiaxial loading. These treatments are similar to static failure criteria for laminates using unidirectional ply data.

2.3.2 Residual Strength Degradation Theories

Most of the currently accepted fatigue life prediction methods for composites are based on residual strength degradation theories. These theories are built upon three assumptions:

1. The static strength can be represented as a two (or more) parameter Weibull distribution.
2. Residual strength after N cycles is related to the initial strength through a deterministic relationship. For example, Sendeckyj presents the following relationship:

$$\frac{d\sigma}{dN} = -\left(\frac{1}{\gamma}\right) f \sigma_a^\gamma \sigma^{1-\gamma}$$

Equation 9

where f and γ are dimensionless functions that may depend on temperature, moisture content, load cycle amplitude, cycle frequency, and cycle shape.

3. Failure occurs when the maximum applied stress equals the residual strength of the laminate as given by the above equation.

Integrating Equation 9 and applying simplifying assumptions (including the previously described assumption 3), the basic residual strength fatigue theory reduces to:

$$\sigma_0 = \sigma_a [1 + (N-1)f]^S$$

Equation 10

where N is the number of cycles to failure under constant amplitude loading σ_a . Finally, including the static strength distribution gives the residual strength distribution as [44]:

$$P(\sigma_r | \sigma_e \geq \sigma_n) = \exp \left\{ - \left[\left(\frac{\sigma_r}{\beta} \right)^{\frac{1}{S}} + \left(\frac{\sigma_a}{\beta} \right)^{\frac{1}{S}} f(N-1) \right]^{\alpha S} + \left(\frac{\sigma_n}{\beta} \right)^\alpha \right\}$$

Equation 11

where $\sigma_n = \sigma_a [1 + (N-1)f]^S$, σ_r is the residual strength, and α and β are the Weibull parameters of the static strength.

The functions f and S can be formulated in many ways based on fatigue test data. For the simplest formulation, $f = 1$ results in a classic power law model. Other formulations are listed in Table 1.

Table 1: Various residual strength degradation fatigue theories from reference 44

Fatigue Theory	S	f
W1	S_0	1
W2	S_0	C
W3	S_0	$C(1-R)^G$
W3A	$S_0(1-R)^G$	$C(1-R)^G$
W4A	$S_0+D(1-R)$	$C(1-R)^G$
W4	$S_0(1-R)^D$	$C(1-R)^G$

Figure 10 is a plot of fatigue theory W3A along with data from tests conducted by Sendeckyj. Note that in this figure, different symbols represent different stress ratios (R).

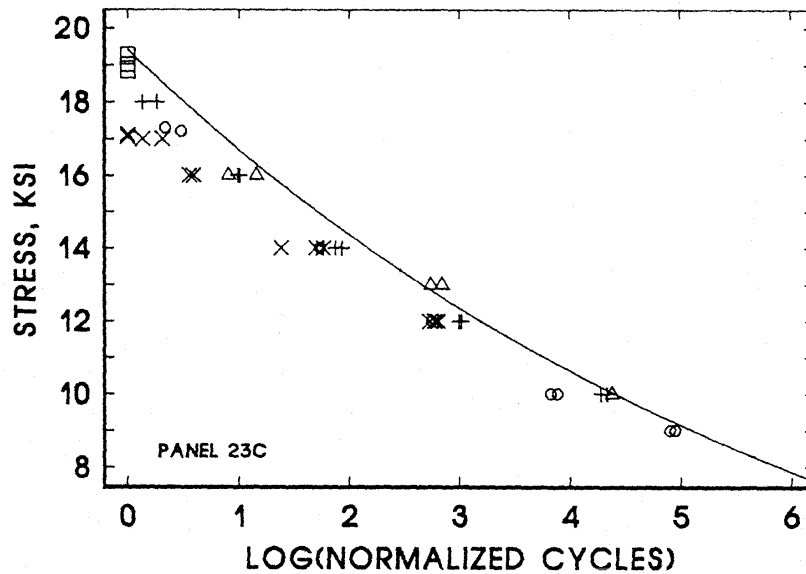


Figure 10: S-N plot of fatigue model W3A and Sendeckyj data [reprinted from reference 44]

A major drawback of residual strength degradation fatigue theories is that after an unknown load history, it is impossible to determine the residual strength without destroying the

laminate. The damage metric is residual *strength*; therefore, destructive testing is required to determine (in this case retroactively) the remaining life of the laminate. Additionally, it is felt that residual strength is not a direct indicator of damage growth. Residual strength generally decreases slowly during most of the laminate life until just prior to failure when residual strength decreases rapidly.

Another drawback is that, as for purely empirical theories, extensive static and fatigue testing for each material system and stacking sequence is necessary to determine the necessary fitting parameters and material constants.

2.3.3 *Stiffness Degradation Theories*

Stiffness degradation fatigue theories make use of the experimental observation that for cross-ply laminates, overall stiffness decreases during cyclic loading. The use of stiffness instead of strength as a damage metric enables non-destructive determination of the damage state, therefore remaining life, of a composite laminate. One such approach developed by Reifsnider et al is based on three assumptions:

1. The fatigue behavior of a laminate is dominated by a *critical element*. This is the primary load carrying ply group, usually the 0° plies.
2. The fatigue life of the critical element can be described using a residual strength degradation theory.

3. Stiffness change during cyclic loading is due to internal load distribution brought about by damage development. This modifies the loads in the critical element, usually increasing them.

For analysis, it is assumed that the maximum applied stress on the critical element is a function of the total applied stress and the instantaneous laminate stiffness. Note that it is assumed that the stiffness of the critical element does not change with cyclic loading. This assumption is based on experimental observations of unidirectional laminate fatigue tests. Using these assumptions, an expression is found for the life of a laminate (.Equation 12).

[44]

$$N = \left\{ - \left[c(\gamma - 1)(N_c - 1) + (1 - c)^{1-\gamma} \right]^{1/(1-\gamma)} \right\} \frac{1}{c}$$

Equation 12

where N_C is the life of the critical element under applied loading σ_{ac} (found from strength degradation fatigue theories); γ is the inverse of the slope of the S-N plot; and c is a linear stiffness degradation rate. The linear stiffness degradation rate is dependent on applied stress as is shown in Figure 11.

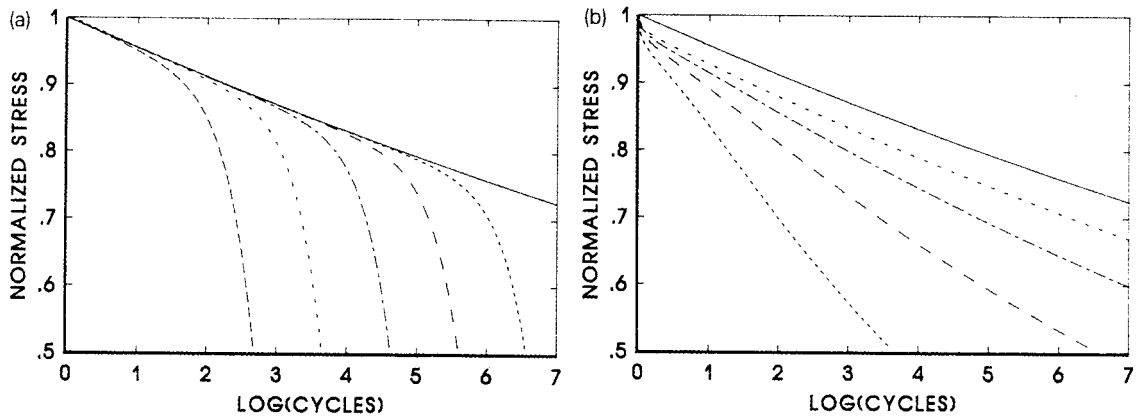


Figure 11: Predicted S-N curved for a [0/90] gr/ep laminate using stiffness degradation theory [reprinted from reference 44]

Stiffness degradation fatigue theories assume that a laminate fails suddenly and globally. Stated differently, when the critical element approaches a critical point, it is assumed that global failure will take place instantly, not considering load sharing and local damage. This has been observed to be a fallacious assumption through experimental observation of unidirectional laminate fatigue tests.

Other shortcomings of current stiffness degradation fatigue theories are that they do not consider lamina thickness and stacking sequence or the occurrence of delamination, all of which can affect damage growth and internal load distribution.

2.3.4 Cumulative Damage Theories

It is rare for a structure to be subjected to a constant amplitude continuous load cycling as the previous theories have been developed to treat. Therefore cumulative fatigue damage theories have been developed to address the problem of multi-stage and spectrum loading.

Cumulative fatigue damage theories fall into two categories: entirely empirical *curve fit* methods, and those based on experimental observation of a damage metric. Many attempts have been made using the latter approach, but have met little success.

2.3.4.1 Equivalent Damage Curve Method

An example of an empirical theory is the Damage Curve method developed by Hashin and Rotem. [12] In this method, damage curves for different load levels are overlaid on an S-N plot for that material. These damage curves define states of equivalent damage due to different load levels. Figure 12 illustrates this theory for two stage loading. The laminate first undergoes n_1 cycles at load level σ_1 which leads to the equivalent damage state (a) then the load level is increased to σ_2 (b). The remaining life is given as the distance between point (b) and the S-N curve.

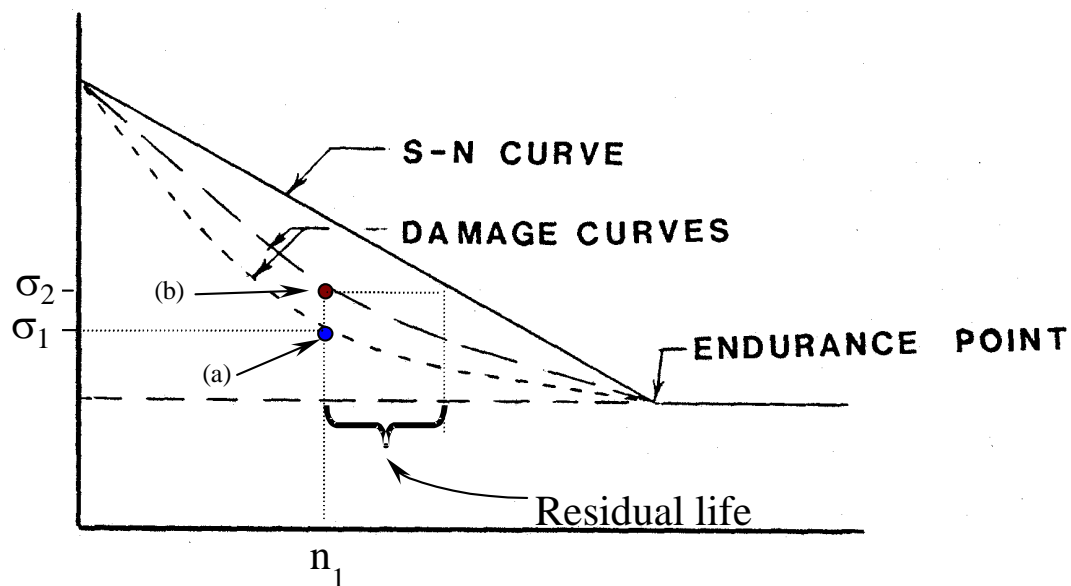


Figure 12: Equivalent damage curve example [12]

Extensive testing is necessary to develop equivalent damage curves and it is impossible to experimentally determine them for all possible loadings. Hashin and Rotem developed a semi-analytical method to predict the shape of the curves while constraining them to pass through two points: static strength at $n=1$, and the endurance point.

2.3.4.2 Cumulative Strength Degradation Method

A cumulative fatigue theory based on experimental damage observation was developed by Broutman and Sahu. [4] This is based on the observation (and assumption) that strength degrades linearly with the number of cycles Equation 13.

$$\frac{d\sigma_0}{dn} = -\frac{\sigma_0 - \sigma_a}{N_a}$$

Equation 13

where σ_a is the applied load and N_a is the number of cycles to failure at that load. This equation can be integrated for a single load stage, or generally for M load stages (Equation 14).

$$\sum_{i=1}^M \frac{\sigma_0 - \sigma_i}{\sigma_0 - \sigma_M} f_i + F_M = 1$$

Equation 14

2.3.5 *Continuum Damage Theories*

The final class of composite fatigue theories is the continuum damage models. In these models, fatigue damage is modeled at the constituent level in order to determine the mechanical response of the damaged laminate and therefore predict damage growth and fatigue life. A continuum mechanics model developed by Talreja [51] is based on the following observations of fatigue damage mechanisms in composite laminates.

1. No single crack governs the response of a laminate. This assumption allows the effect of matrix microcracks to be smeared out to a locally homogenous field.
2. Damage develops along preferred orientations. Matrix cracks have been observed to develop either parallel or perpendicular to the local fiber direction. If crack orientation significantly affects the mechanical response of the laminate a second-order or higher tensor field is required to adequately characterize damage. If a restriction to small deformation is imposed, a vector field characterization is sufficient.

Using these assumptions, Talreja has developed a continuum model to represent damage in a composite laminate. Due to the length and intricacy of the model it is inappropriate to present in this review; therefore the interested reader is referred to reference [51] for a full explanation.

This model, or any other continuum damage model, has *not* been successfully applied to fatigue loading situations of composite laminates. This is due to the mathematical

complexity of the models making cyclic evaluation and damage summation unwieldy or impossible.

2.4 Micromechanics-based Fatigue Models

Several micromechanics-based tensile fatigue models have been developed for a variety of fiber-reinforced materials. [3,10,25,32,45] This section presents several of these models that are pertinent to the focus of this work.

2.4.1 McLaughlin Theory for Uniaxial PMCs

Based on the idea that the load transfer between the fibers and the matrix determines the tensile strength of unidirectional composites, McLaughlin developed a fatigue life prediction method for unidirectional composites using a fracture-mechanics approach for calculating fiber/matrix interface damage growth and a chain-of-bundles method for predicting tensile failure. The central idea in this theory is that tensile fatigue loading causes fiber/matrix interface damage resulting in growth of the ineffective length. Following the chain-of-bundles type of failure criterion, the ultimate tensile strength of the composite is therefore reduced.

This theory states that fatigue failure will occur when the ineffective length grows to a critical value. The “critical value” of the ineffective length, δ_f (Equation 15), is calculated using the Rosen chain-of-bundles theory discussed previously in section 2.2.2. In this equation, α and β are the Weibull distribution parameters for the *fiber* strength, and σ_{\max} is the maximum cyclic mean fiber stress.

$$\delta_f = \frac{1}{\alpha\beta e} \sigma_{\max}^{-\beta}$$

Equation 15

The growth of the fiber/matrix interface failure zone is modeled using a Paris-type of crack growth equation where C_σ and m are empirically derived constants (Equation 16).

$$\frac{da}{dN} = C_G (\Delta G_2)^{m/2} = \frac{1}{2} C_\sigma (\Delta \sigma)^m$$

Equation 16

The result of McLaughlin's theory for constant amplitude tension-tension fatigue loading is shown as Equation 17. In this equation, the first term represents the critical ineffective length calculated from the fiber strength statistics using the chain-of-bundles failure criterion. The second term represents the contributions to the ineffective length from elastic deformation and fiber/matrix interference. Finally, the right-hand-side term is an expression for the cumulative fiber/matrix interface failure length after tension-tension fatigue loading.

$$\frac{(\sigma_{\max})^{-\beta}}{\alpha\beta e} - \delta_E \left[1 + \frac{1}{\eta} \left(\frac{\sigma_{\max}}{S_T} - 1 \right) \right] = C_\sigma (\Delta \sigma)^m (N - N_i)$$

Equation 17

This equation requires *ten* individual material inputs:

- Fiber elastic and geometry properties: E_f , ν_f , and d_f
- Weibull fiber strength parameters: α and β
- Matrix and fiber/matrix interface elastic and failure properties: G_m , T , η
- Fiber/matrix interface crack growth parameters: C_σ , m

The major shortcoming of this theory is that the heart of the model, the fiber/matrix interface crack growth equation (Equation 17, RHS), is empirically derived. McLaughlin notes that values for C_{σ} and m “could not be found, but they can be calculated from constant-amplitude fatigue data.” Such methodology negates the usefulness of the theory as it is essentially reduced to an elaborate curve fit.

2.4.2 *Efficiency of the Fiber-Matrix Interface Fatigue Theory*

In 1994, Subramanian published a paper focusing on the significance of the fiber-matrix interface on the fatigue life of PMCs. [49] The central concept in that model is the inclusion of an empirical parameter called the *efficiency of the interface* to describe the effectiveness of fiber-matrix load transfer. The ultimate strength of uniaxial PMCs is assumed to be controlled by the fiber-matrix interface, and therefore can be characterized by the efficiency of the fiber-matrix interface. Subramanian combines observations to note that the efficiency of the interface, and therefore the strength of the laminate, tends to decrease with cyclic tensile loading. From this observation a fatigue life model based on the degradation of the efficiency of the interface is proposed.

2.5 Research Needs / Literature Summary

Although there are tools currently used for fatigue life prediction of composite laminates, they are largely empirically based *rules* and require experimental fatigue life data for each specific material, loading, and environmental condition. Furthermore, there exists a lack of a complete fundamental understanding of the fatigue process in polymer matrix

composites. A critical area that is not well understood is the fatigue process that occurs in uniaxial laminates. Although uniaxial laminates are rarely used in practical applications, the fatigue life of the axial (or near-axial) plies controls the fatigue life of a more general angle-ply laminate according to the widely accepted critical element theory. As such, understanding and accurately modeling the fatigue behavior of the uniaxial composite forms the foundation for more comprehensive fatigue life models.

In a report by the National Materials Advisory Board that critically examined the state-of-the-art in fatigue life analysis for PMCs, they conclude that there is a clear need for a “lifetime prediction method based on the structural material or element level.” [30] That need still exists today.

CHAPTER 3: EXPERIMENTAL

As part of this work, an experimental test program was conducted to explore the tension-tension fatigue behavior of uniaxial composite specimens. This test program included quasi-static tensile strength tests, tension-tension fatigue life tests, and residual strength tests after fatigue loading. This chapter describes the materials, equipment, and procedures, used in the experimental testing, and then presents the basic results.

3.1 Objective

The overall objective of the experimental test program was to gather data on the tension-tension fatigue behavior of a uniaxial composite laminate for comparison to various analytical models. Both quasi-static tension and tension-tension fatigue tests were performed.

3.2 Coupon Description

3.2.1 Test Material

The polymer matrix composite material system selected for testing was IM7/8552 manufactured by Hexcel Corporation. This material is typical of the high performance grade carbon fiber reinforced thermoset composites used in the aerospace industry. IM7 is a continuous, high performance, intermediate modulus PAN-based carbon fiber. The 8552 matrix is a toughened thermosetting epoxy resin system designed for structural applications

that require high strength, stiffness, and damage tolerance. Typical properties of the fiber, matrix, and composite are given below.

Table 2: Manufacturer's published properties for Hexcel IM7/8552.

	IM7 Fiber Properties	8552 Cured Resin Properties	Typical Cured Composite Properties
Tensile Strength (Mpa)	5,150	120.7	2760
Tensile Modulus (Gpa)	276	4.67	168
Density (g/cc)	1.78	1.301	
Ultimate tensile strain, %	1.81	1.70	
Fracture toughness, K_{IC}, ksi $\sqrt{\text{in}}$		1.475	
Strain energy release rate, G_{IC}, in-lb/in²		3.88	
Fiber volume fraction			0.60

3.2.2 Coupon Configuration

The individual test coupons were two-ply, uniaxial laminates ($[0_2]$) that were 305 mm total length, 200.3 mm gage length, 12.7 mm wide, and 0.356 mm thick. A drawing and photograph of a typical specimen are shown in Figure 13.

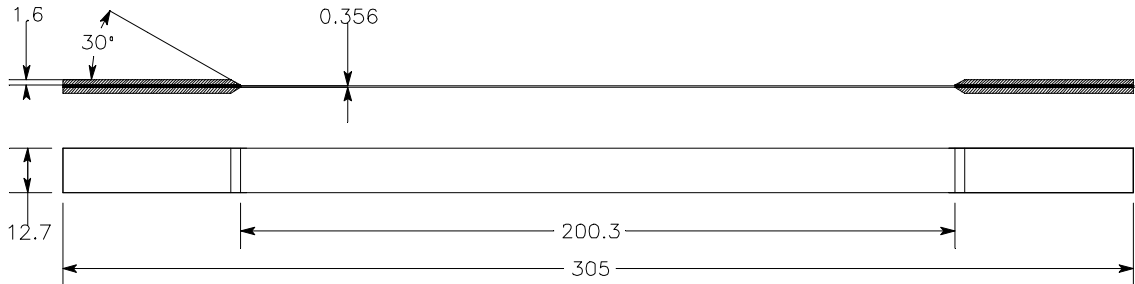




Figure 13: Drawing and photograph of a test specimen (dimensions shown in mm).

3.2.3 Coupon Fabrication

Approximately 120 $[0^{\circ}_2]$ individual test coupons were fabricated using Hexcel IM7/8552 unidirectional graphite/epoxy pre-impregnated tape. These specimens were fabricated in two distinct batches (the first in May 2001 and the second in August 2002), but both were the same $[0_2]$ layup, were fabricated from the same lot of IM7/8552 unidirectional tape, and were cured using the same cure cycle, equipment, and procedures. However, the two batches differed in the materials and procedures used for bonding the reinforcement tabs. This difference (detailed below) turned out to greatly impact on the tensile static and fatigue performance of the specimens.

For each batch of test specimens, four 305 mm by 356 mm $[0^{\circ}_2]$ laminates were laid up using Hexcel IM7/8552 unidirectional graphite/epoxy pre-impregnated tape. After the laminates were laid up, they were placed on a large aluminum cure plate and surrounded cork dams. Separate aluminum caul plates were then placed over each laminate. Bleeder cloth was not used because the IM7/8552 material is supplied as a net resin system having

a cured fiber volume fraction of 0.60. A vacuum bag was put over the assembly to prepare for autoclave cure. The vacuum-bagged assembly was then loaded into the autoclave and cured according to the manufacturer's recommended cure cycle, data from which is given in Figure 14.

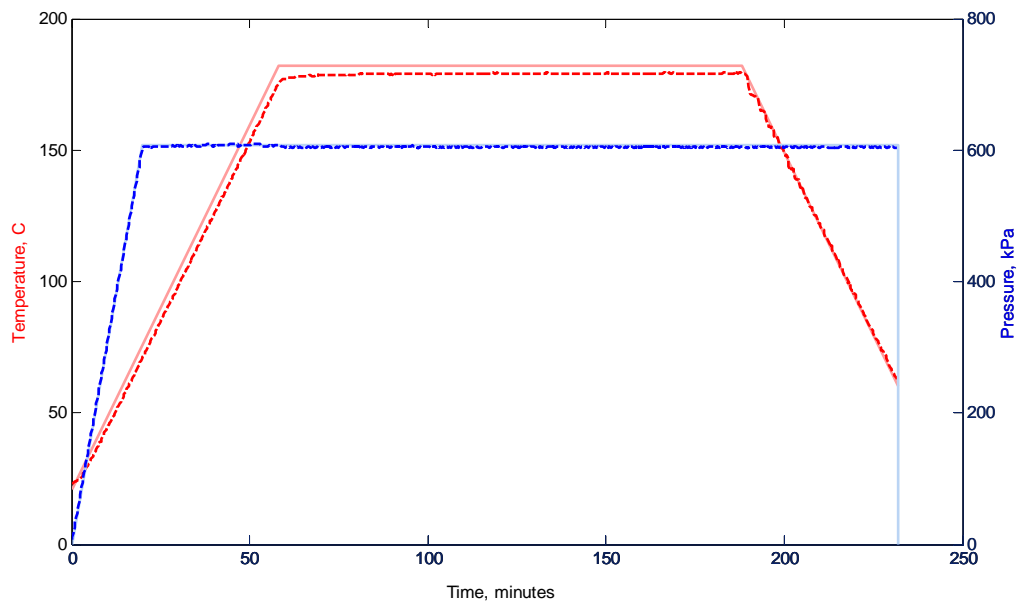


Figure 14: Test specimen cure cycle data from cure on August 8, 2002.

After the test laminates were cured fiberglass strips were applied to the edges of the laminates to reinforce the region of the specimens that would be gripped in the test machine as per ASTM standard D-3039 (Standard Test Method for Tensile Properties of Polymer Matrix Composite Materials) and D-3479 (Standard Test Method for Tension-tension Fatigue of Polymer Matrix Composite Materials). The tab material was 1.6 mm thick G-10 fiberglass laminate and the edge closest to the gage section of the specimens was beveled at 30°. For the first batch of test specimens, the reinforcement tabs were bonded onto each

laminates using Hysol 9309.3 2-part paste adhesive cured at room temperature using steel weights for pressure. For the second batch of specimens the reinforcement tabs were bonded to the test laminate using Cytec FM-123 film adhesive. The tab/FM-123/laminate assembly was sandwiched between aluminum caul plates, vacuum bagged, and oven cured at 121°C under full vacuum resulting in approximately 100 kPa pressure on the FM-123 adhesive.

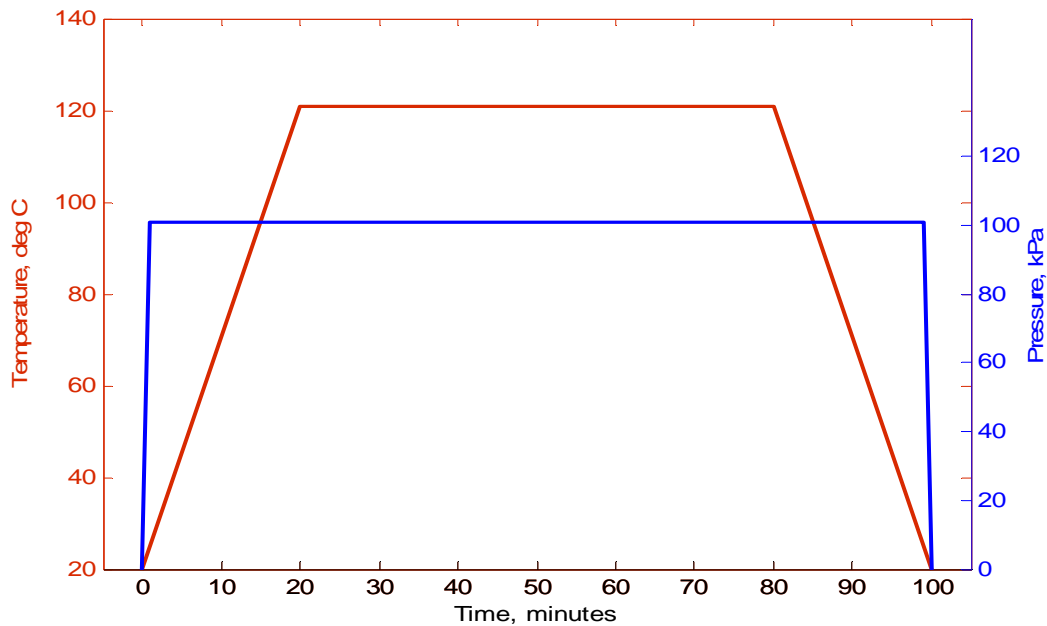


Figure 15: Test specimen Batch B tab bond cure cycle

3.3 Experimental Testing

A total of 43 quasi-static tension tests and 47 tension-tension fatigue tests using two batches of test coupons were completed in this experimental test program. All tests

conducted using the batch A specimens were invalidated due to poor consistency in the adhesive bond between reinforcement tab and the test laminate. Tests completed using the batch B specimens were valid and yielded useful and consistent data.

3.3.1 Test Specimen Batch A

After completing a set of 12 quasi-static tests and 16 fatigue tests using the first batch of specimens, the data was closely examined for validity, consistency, and correlation with the model. Surprisingly, the data showed no observable trend in the fatigue life behavior.

The first batch (batch A) produced very wide scatter in early fatigue tests. Specimens were closely examined and it was found that the bond between the reinforcing tabs and the specimen was inconsistent and of poor quality. As previously stated, for batch A test specimens, the reinforcement tabs were each bonded onto the test laminate specimen using Hysol 9309.3 2-part paste adhesive and dead weight pressure. Post-facto detailed examination of specimens from batch A revealed frequent instances of large voids, unbonded regions, and inconsistent thickness of the adhesive bond. In addition, the parallel tolerance between the tabs and the test laminate itself was found to be excessive. This poor quality adhesive bond resulted in inconsistent load transfer from the tab to the test laminate (due to the adhesive voids), and misalignment of the specimen in the test machine grips (due to the poor parallel tolerance). These problems invalidated all tests using the batch A specimens, and the data from those tests was not used in the remainder of the program.

3.3.2 Test Specimen Batch B

In light of the experience gained during the testing of batch A specimens, each specimen from batch B was inspected for consistency of the tab adhesive bond and parallel tolerance of the tabs and the test laminate prior to testing. For a specimen to be qualified, the adhesive bond between the tab and the laminate could not have any voids or dis-bonds visible to the naked eye, and the parallel tolerance between the tab faces had to be within 0.02 degrees (equivalent to a thickness variation of 1 mm over the tab length). Data from quasi-static tests using the batch B specimens showed reduced scatter and an increase of measured strength. The data gathered during the testing of these specimens is considered valid and was correlated with the fatigue life model developed in this work.

3.3.3 Equipment Description

All testing was performed on a MTS model 810, 55kip uniaxial hydraulic test frame equipped with hydraulic wedge grips and computer data acquisition. The test machine was controlled by a MTS model 458.20 control system in concert with a personal computer.

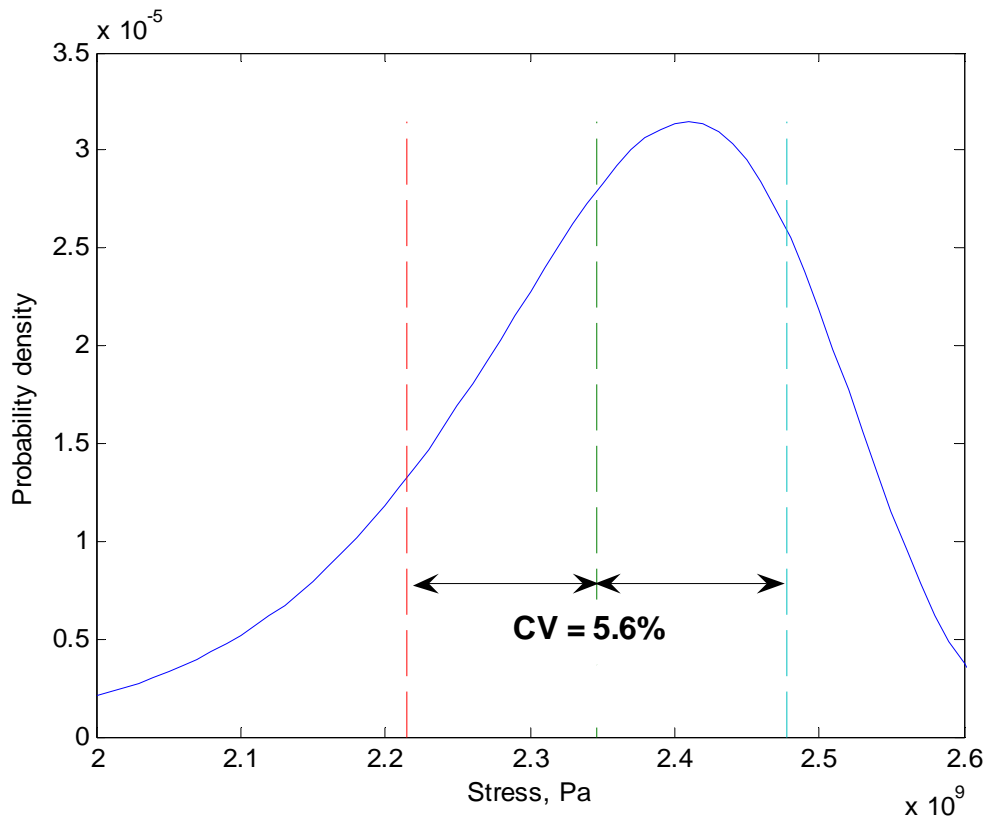
3.3.4 Quasi-static Testing

Ten coupons were tested under quasi-static tension loading. These static tensile tests were conducted according to ASTM D-390 to measure the static ultimate tensile strength of the test coupons. Testing was conducted in displacement control at a constant stroke rate of 0.25 mm/min resulting in an equivalent strain rate of 500 μ strain/s. Throughout the test load and cross-head displacement data were sampled at 4 Hz by the personal computer data

acquisition system. Tests were stopped when the specimen no longer carried any load (catastrophic failure). The results are presented in Table 3 and the associated Weibull distribution functions are plotted in Figure 16.

Table 3: Quasi-static tension test results (specimen batch B only)

Number of Specimens	10
Mean Strength (Gpa)	2.346
Std. Deviation. (Gpa)	0.131
C.V.	5.62%
Weibull Parameters, SI units	
Beta	18.63
Eta (Pa)	2407540951
Alpha (=1/Eta)	4.15362E-10



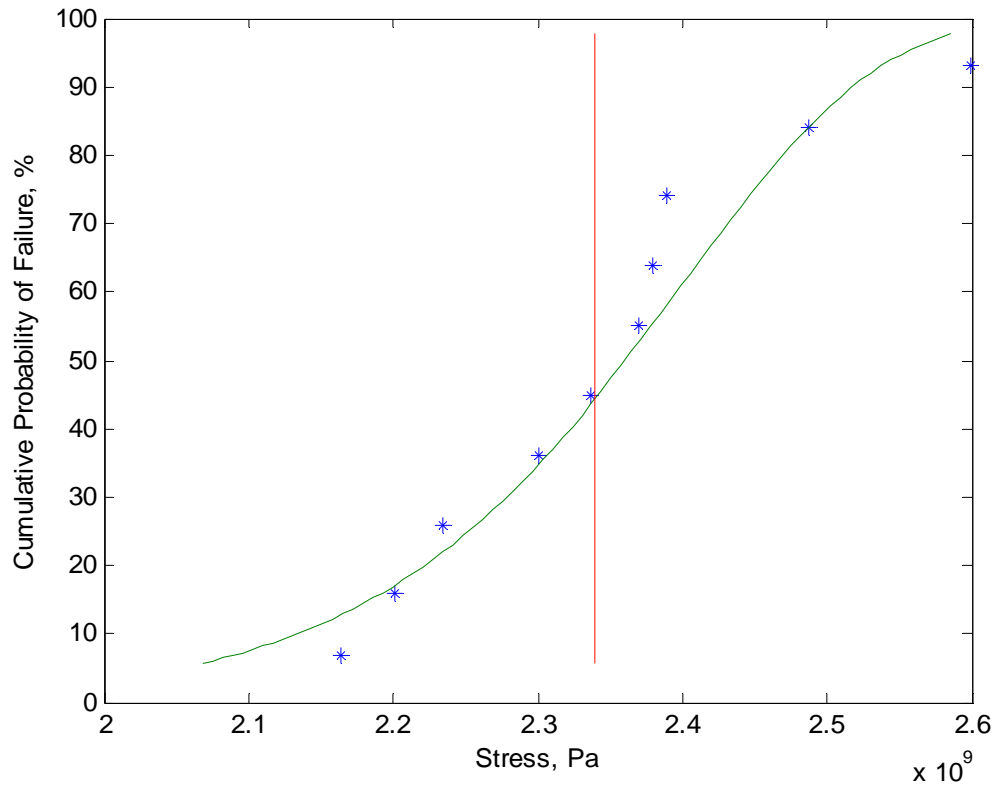


Figure 16: Weibull probability density function and cumulative probability for static test data of batch B specimen tests

3.3.5 Fatigue Testing

Fatigue life tests were performed to experimentally measure the tension-tension fatigue life of the test laminates. The test coupons used for fatigue testing were the same configuration and from the same batch as the coupons used for static strength testing.

All fatigue tests were run under load control with a constant amplitude sinusoidal load profile and a load ratio (R) of 0.1. The peak cyclic load was selected prior to each test as a fraction of the mean static strength as measured from the quasi-static test series. The precise value for the peak load was calculated individually for each specimen according to

its measured dimensions. This method enabled the S load (based on the measured mean strength) applied to each specimen to be accurate within 0.3%.

A total of 31 fatigue tests were performed using batch B specimens. Of these tests,

- 20 were successful fatigue tests for S_{ave} from 0.93 to 0.95
 - 15 specimens failed during fatigue loading
 - 5 specimens reached 100,000 cycled without failing
- 4 were non-qualifying fatigue tests. Tests were disqualified either because of machine difficulty resulting in unintended or unknown loading (2 tests) or fatigue failures where the fracture line is within 5 mm of the reinforcement tab (2 tests).
- 7 were residual strength tests. In these tests the specimen was subjected to a pre-determined number of tension-tension fatigue load cycles and then it was loaded quasi-statically until failure.

During each fatigue test the maximum and minimum cyclic load as displayed on the MTS console were recorded and load and stroke data was sampled at periodic intervals (see Figure 17 for an example). No strain gages or extensometers were used during fatigue tests. However, load and stroke data for a complete load cycle were recorded at intervals throughout each fatigue test. Both the MTS console and the data acquisition computer independently recorded the total number of load cycles.

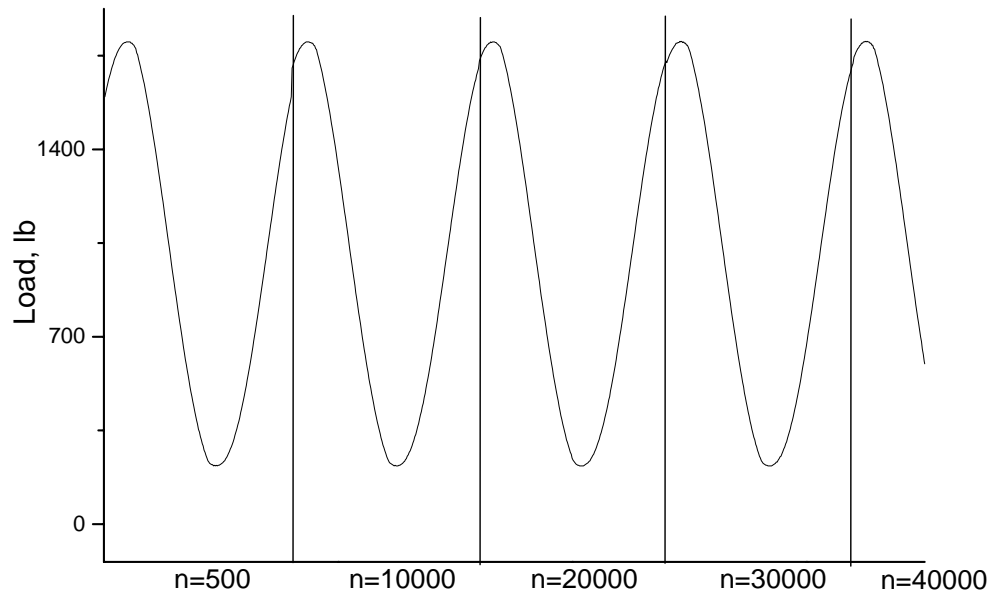


Figure 17: Load history recorded during testing (specimen H-121). The period for each cycle is 0.75 seconds. Load and stroke data was taken periodically during the testing and later examined to verify test integrity and validity.

All fatigue tests were performed using the same test equipment described in the previous section. Extra care was taken to ensure true axial alignment of each specimen when gripped in the test machine. The use of alignment jigs attached to the grip blocks and a square for checking the actual specimen alignment enabled consistent specimen alignment of 0 deg with a maximum error of 0.1 deg. This alignment was critical to ensure that the applied loading was in the axial direction because non-axial loading leads to a multi-axial stress state in the composite material.

The basic $S-N$ results from the 20 valid fatigue-life tests are given in Table 4 and in Figure 18. In this plot the ordinate is labeled as S_{AVE} to emphasize that the applied loading is based

on the average strength for a population of specimens because knowledge of the precise strength of any particular specimen is impossible to obtain without destructive testing.

Table 4: Fatigue Test Summary

S	Total Valid Fatigue Tests	Number of Runout Tests	Fatigue Failures
0.93	8	3	N = 38, 3040, 6498, 11081, 50515
0.94	6	2	N = 1086, 1267, 2626, 3227
0.95	6	0	N = 185, 353, 916, 2592, 6130, 16781

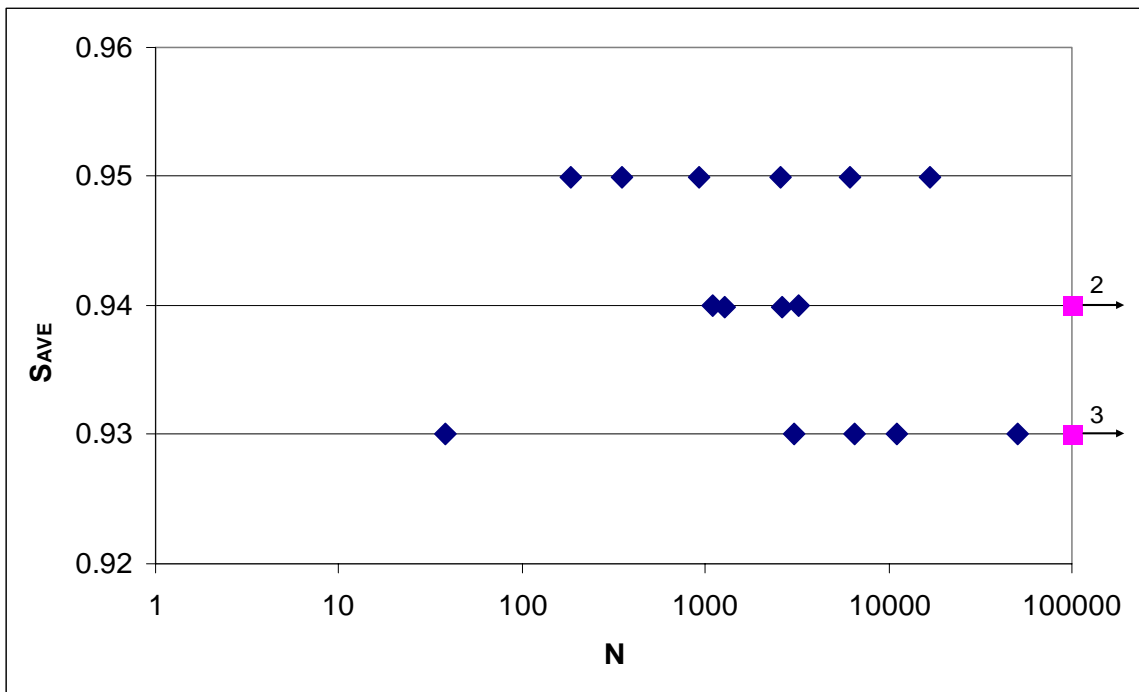


Figure 18: Fatigue test data for the 20 qualifying fatigue tests. The pink squares represent specimens that did not fail before reaching the runout criterion of 100,000 cycles.

CHAPTER 4: THEORETICAL MODEL

4.1 Overview

As mentioned in section 1.3, a major limitation of current fatigue life prediction methods for PMCs is that they fundamentally rely on experimentally derived S-N data for unidirectional plies to characterize property degradation and fatigue failure for more complex laminates. Although the physical damage mechanisms responsible for fatigue behavior have been identified, there is no well-demonstrated method for analytical prediction of the S-N curve for unidirectional laminates. As a result, the fatigue behavior for particular material systems is generally characterized by a variety of empirical curve fits, two examples of which are shown in Figure 19. These fits suffer from the fact that they are not based on the physical mechanisms responsible for fatigue damage and failure. As such, they neither provide insight into the mechanisms of fatigue nor offer analytical capabilities to predict the fatigue performance for different conditions or material systems. Supporting this argument is the fact that most curve fits do not include a fatigue damage growth threshold and are thereby in stark disagreement with the collective observation that PMCs clearly exhibit a damage growth threshold. Finally, the single curve fit approach to characterizing fatigue does not address the wide scatter of fatigue life data that is typical of high performance uniaxial composite laminates.

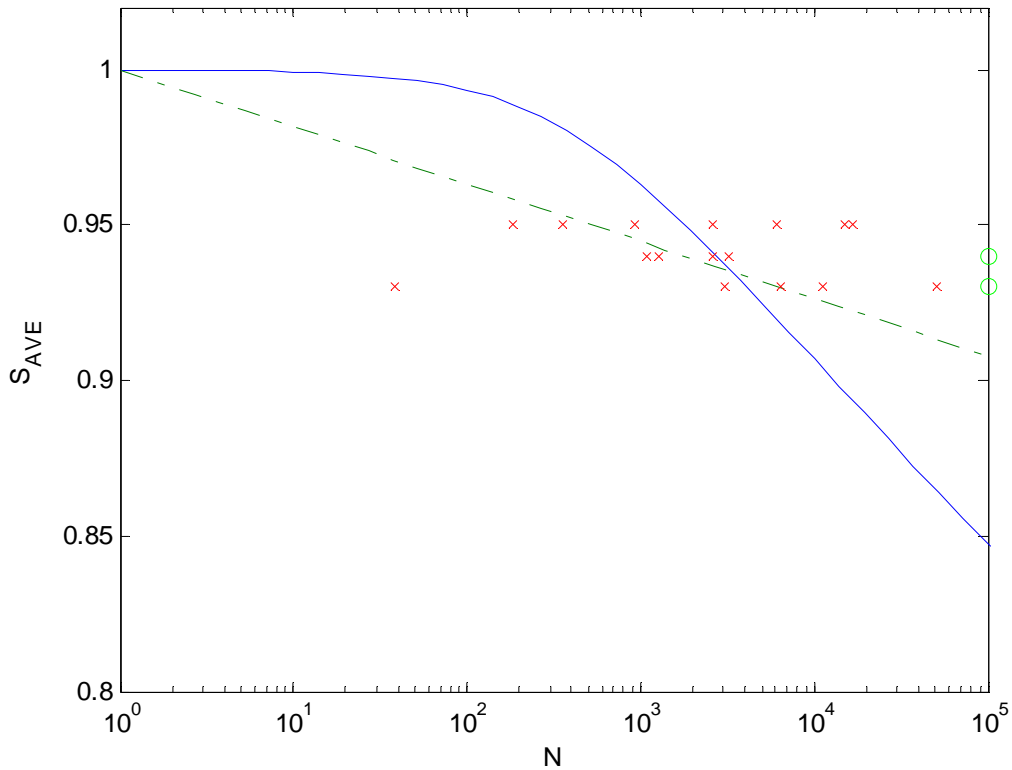


Figure 19: Experimental data compared to residual strength fatigue theory given by Equation 10 (blue line) and a traditional log-linear fit. Note that these fits are purely empirical and are not based on physical damage mechanisms. Also note that the fits do not indicate a fatigue damage growth threshold.

After reviewing the state-of-the-art in fatigue analysis methods for polymer matrix composites (PMCs), the development of a mechanism-based model that characterizes the tension-tension fatigue life behavior of uniaxial PMCs was selected as the primary goal of this work. In addition to being based on the physical damage mechanisms responsible for fatigue damage growth and failure, the use of any empirical S-N data was to be strictly

avoided so that the resulting model could be used to predict fatigue behavior without requiring experimentally derived fatigue life fitting factors.

An ideal fatigue life theory for PMCs would be based on the physical mechanisms that are responsible for property degradation and failure of PMC laminates as a result of fatigue loading. However, this ideal is made impossible because of the great complexity of real composites. Although the modern computational power available makes it possible to model a complete composite down to the fiber/matrix scale, real application of such modeling is impossible (or at least impractical) because of the sheer quantity of unknowns in real composites. Despite the tremendous improvements in composite manufacturing methods and quality control, there is still substantial variation in the micro-structural arrangement of real composites. As will be discussed in section 4.3, the fundamental mechanisms responsible for fatigue in composites are rooted at the micro-structural fiber/matrix level. Consequently, a useful micro-mechanics based model for the fatigue analysis of composites would require knowledge of the composite down to the fiber/matrix scale at every point in the entire volume of the composite. Because this is impossible or impractical, micro-mechanical models alone are not sufficient for modeling or predicting the behavior of real composites.

The model developed in this work uses non-deterministic methods as a bridge to enable a micro-mechanical damage growth model to be applied to the macro-mechanical performance of a composite laminate. The statistical model is based on the chain-of-bundles type of tensile strength model and uses the distribution of static test data as a key

input. The micro-mechanical damage growth model uses fracture mechanics to model fiber/matrix interface damage growth. By combining statistical analysis with micro-mechanical modeling, this model enables prediction of the tensile fatigue performance of a uniaxial PMC using only basic material properties and static test data as inputs.

4.2 Scope and limitations

The model developed/described in this dissertation addresses the fatigue performance of high-performance polymer matrix composites typical of those used in aerospace applications. In this class of materials, the reinforcement fibers are long (thousands times longer than their diameter) and their strength and stiffness is much greater than that of the polymer matrix. Furthermore, the model developed in this dissertation only applies to unidirectional composites under axial tensile fatigue loading. However, as discussed previously, this case is of specific interest because the tensile fatigue performance of uniaxial lamina is the dominant factor for tensile fatigue of more general laminates.

The discussions and analysis presented in this chapter focus on axial tension-tension fatigue of uniaxial long fiber reinforced polymer matrix composite laminates. Therefore, for the sake of brevity, all references to *fatigue* throughout this chapter refer to axial tension-tension fatigue of uniaxial polymer matrix composite laminates.

4.3 Physical Foundations

The fatigue life prediction model developed in this work consists of three parts corresponding to the top-level stages of fatigue life: initial damage (or damage initiation),

damage growth, and failure. This section defines the three key physical concepts on which the fatigue theory developed in this dissertation is based.

4.3.1 *Initial Damage*

The first key physical basis of this model is that *real composites contain flaws*.

A fundamental characteristic of all real engineering materials is that, at some scale, they contain flaws. In this context, a *flaw* is broadly defined as any characteristic of the real material that differs from the idealized engineering material model. For example, in engineering calculations strength-of-materials models treat metals as homogenous, isotropic materials. However, in reality they will actually contain many small variations in micro-structure, chemical composition, or geometry. The general engineering strength-of-materials type of models commonly used in composite analysis disregard these subtle variations because they are assumed not to have an effect on the observed material performance. However, this research suggests that flaws, even those at the microscopic fiber/matrix scale, play a key role in the actual performance of the material because they can lead to fracture-type failures.

Fracture mechanics methods have been developed to account for the effects of these non-ideal, semi-random material variations or flaws in metallic structures. However, there is no similar generalized theory that allows the designer or analyst of fiber-reinforced composite structures to account for the affects of non-ideal material properties or characteristics. The general reason for the lack of such a theory is the innate heterogeneity and complexity of

fiber-reinforced composites. Therefore, understanding of the types of flaws present and their relative impact on the integrity of a PMC is the first step in the development of mechanism-based model for fatigue of PMCs.

The general model of long-fiber polymer matrix composites idealizes a composite as evenly distributed, continuous, consistent fibers that are perfectly bonded to a void-free, homogenous polymer matrix. In reality this is not the case. There are many ways that the actual composite differs from this ideal model, and these differences affect the integrity and performance of the composite.

For any sort of progressive damage to occur, such as fatigue damage, there must be a physical variation within the material at some level that gives rise to internal stress/strain variations. In traditional fracture-mechanics based analysis of fatigue in metals, this variation is the “defect” which can be a crack, void, or inclusion. The defect causes increases in local stresses which can lead to its growth for certain global loading cases. In PMCs, the variation (“flaw”) can take many different forms such as matrix voids, fiber ends (or breaks), matrix micro-cracks, fiber/matrix debonds, fiber discontinuities, fiber orientation variations, fiber packing variations, or fiber strength variations (see Figure 20). One of the main results of these built-in flaws is that they cause the internal stress state in the composite to vary from point to point when the composite is loaded. This is analogous to how flaws (at the micro or macro scale) in metals cause local stress concentrations. In other words, the flaws give rise to local stress concentrations within the composite causing

the stress/strain state within the PMC to be significantly different from and more complex than that in the idealized continuous fiber reinforced polymer matrix composite model.

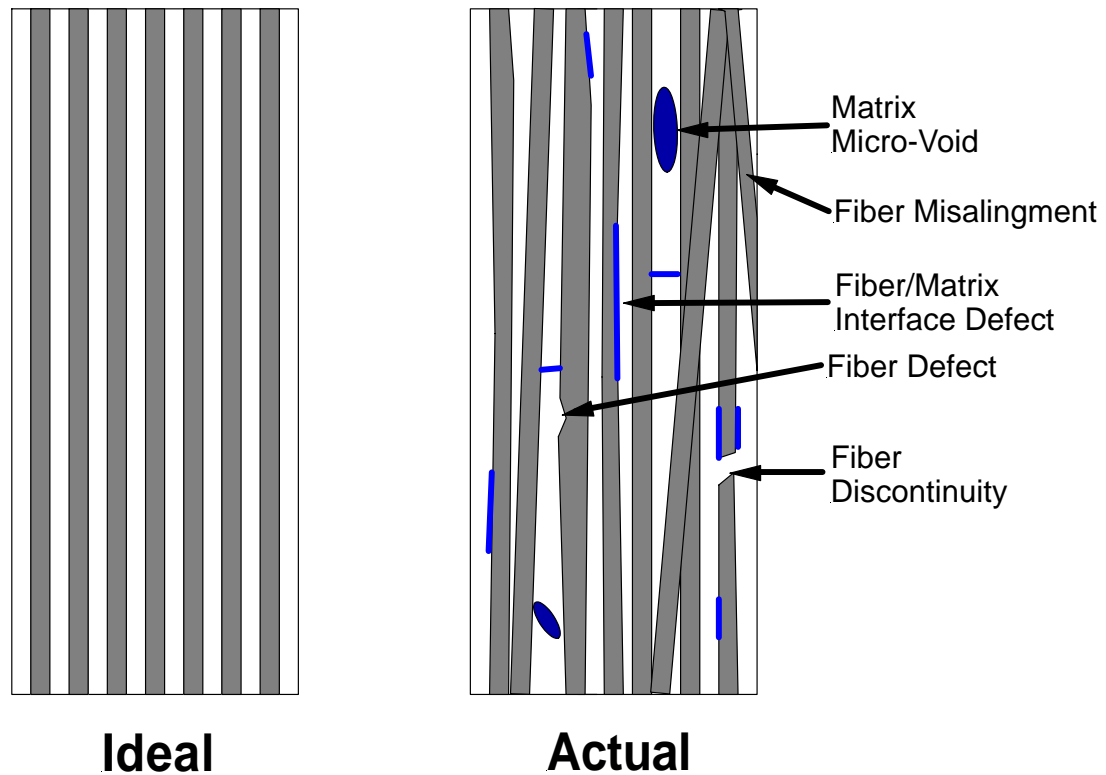


Figure 20: Qualitative illustration of the idealized unidirectional composite model and typical defects found in actual composites.

Upon loading, these local stress concentrations can lead to further damage such as matrix cracking and local fiber failures. Under static loading conditions the macro-scale effects of these micro-failures are mitigated by the load sharing between fibers provided by shear transfer through the matrix. However, under high stress cyclic loading they become initiation sites for fiber-matrix interface damage.

In summary, although a virgin composite might not have a significant amount of fiber discontinuities or initial fiber-matrix interface damage, the occurrence of micro-scale stress concentrations caused by “built-in flaws” leads to the initiation and growth of a great deal of additional damage, which is the subject of the next section.

4.3.1.1 *Effect of Initial Damage on Strength*

One key illustration of the initial damage state of a laminate is to compare the rule-of-mixtures calculated value for the longitudinal strength of a particular material to the actual strength measured through testing. The rule-of-mixtures equation for longitudinal static strength (Equation 18) uses the *mean* individual fiber strength to calculate the laminate strength and assumes that all the fibers are identical, continuous, perfectly spaced, perfectly aligned, and perfectly bonded to a flawless matrix. Thus, the rule-of-mixtures prediction represents the *ideal* composite whereas in reality, there are a variety of physical differences between an ideal composite and an actual composite. The quantitative effects of these differences can be interpreted as representing the initial damage state of the laminate. For the material used in this study (see section 3.2.1), the strength predicted by the Rule-of-Mixtures is **33%** greater than the manufactures quoted strength for the cured laminate.

$$\sigma_{comp}^{ult} = \sigma_f^{ult} V_f + \varepsilon_f E_m (1 - V_f)$$

Equation 18

4.3.1.2 *Problems and Limitations of the Rule of Mixtures Strength Prediction*

The ideal strength prediction such as that given by the Rule-of-Mixtures model has several major shortcomings. First, fiber strength is more accurately characterized by a somewhat

wide distribution rather than a single value, often represented by a Weibull distribution (as shown in Figure 21 and discussed in the Literature Review). As such, the rule-of-mixtures neglects potential effects of the fiber strength distribution to simplify the strength estimation calculation.

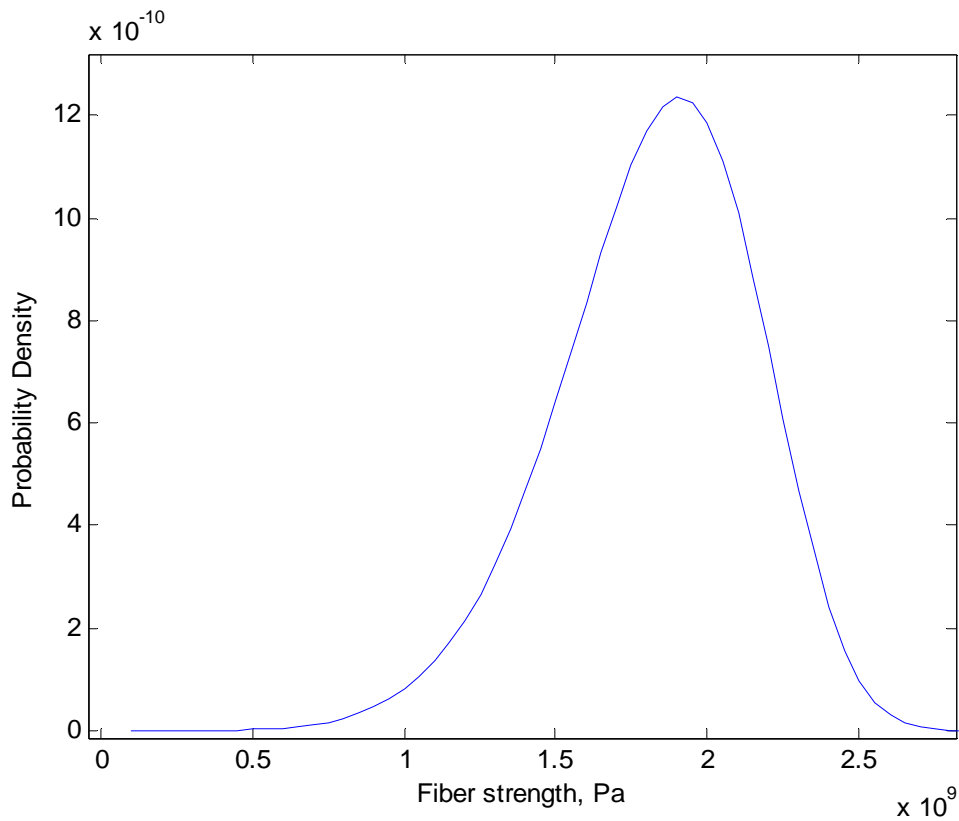


Figure 21: A typical fiber strength distribution. The values used in the distribution shown here are for the carbon fibers from the work of McLaughlin [Reference 25]

A more serious shortcoming of the rule-of-mixtures type of strength equation is that the fiber strength value used for analysis often does not reflect the strength of the fibers in the as-manufactured composite. Fiber strength tests are typically performed under well-controlled laboratory conditions where the fibers are carefully handled. In contrast, the

fibers in the laminate are subjected to a variety of additional processes, such as spooling, pre-pregging, shipping, layup, and high temperature pressure cure. These processes invariably cause some damage to the fibers and result in a decrease of the mean fiber strength and a potential broadening of the fiber strength distribution.

The result of the differences between the ideal single-value representation of fiber strength and the actual performance of the fibers in composite laminates contributes to the poor correlation of the rule-of-mixtures strength model and the actual measured strength of real unidirectional composite laminates. This is because it is based on the idealized model of unidirectional composites that does not adequately reflect the complex nature of unidirectional composites.

4.3.2 *Damage Growth*

The second key physical basis for the model developed in this dissertation is that *tensile cyclic loading above a certain threshold causes local damage to grow*. In the previous section it was established that composite laminates contain many small internal flaws or defects. This section will qualitatively explain the critical damage modes for unidirectional composites under tension-tension fatigue loading and how that damage grows as a result of fatigue loading.

Several types of damage can develop as a result of cyclic uniaxial tensile loading, however, the damage type both grows as a result of cyclic loading *and* directly affects the uniaxial

tensile strength of PMCs is *fiber/matrix interface damage* (see Basis 3 for how this affects tensile strength). Fiber/matrix interface failure can be initiated as the result of many types of other local damage such as transverse matrix (micro) cracks, fiber fractures, or interface damage. During the first loading cycle, many of these types of local damage sites are created due to the stress concentrations created by flaws or discontinuities in the composite (as described in the previous section). In fact, during tension-tension fatigue loading almost all local damage types eventually lead to local fiber-matrix interface damage!

The goal of the damage growth model is to calculate the growth of the fiber/matrix interface failure length at each damage site as a result of cyclic tensile loading. This model must also incorporate a damage growth threshold (mean stress level) below which the damage does not grow. To accomplish this, a micro-mechanical linear elastic fracture mechanics model of the fiber/matrix bond was developed. This model is explained in section 4.4.4.

4.3.3 *Fatigue Tensile Failure*

The third key physical assumption in this model is that *tensile failure occurs when the fiber/matrix interface damage density grows to a critical value.*

The tensile failure criteria used in this model follows from the chain-of-bundles family of models. Briefly, because the fibers in real composites are neither continuous nor consistent along their length, the uniaxial tensile strength of a composite is determined by both the

strength of the fibers themselves *and* the efficiency of load transfer between the fibers and the matrix.

The previous section discussed the assumption that fiber/matrix interface damage grows as a result of cyclic tensile loading. The result of fiber/matrix interface damage is an *increase* of the ineffective length. Relative to the integrity of the whole composite, the increase in ineffective length reduces the fiber/matrix load transfer efficiency and therefore decreases the composites ultimate tensile strength. Therefore it can be stated that fatigue loading causes an increase in ineffective length which results in a decrease of the tensile strength of the composite laminate. When the laminate's tensile strength is reduced to equal or less than the maximum applied cyclic load, the composite fails.

4.3.4 Limitations of Chain-of-bundles Models

The chain-of-bundles family of tensile strength models uses the fiber tensile strength distribution alone to characterize the initial damage state of the composite. This approach contains several major implicit assumptions. First, it assumes that the fibers are not damaged or affected during the various stages of manufacturing such as pre-pregging, layup, and cure. The strength distribution of the fibers themselves is measured through testing short lengths of bare fibers under carefully controlled laboratory conditions. In contrast, the fibers in an actual composite structure have likely undergone several stages of manual and machine handling during which they can be damaged through abrasion or kinking (small radius bending). Additionally, the fibers in composite structures are much

longer than the fiber lengths used for bare fiber strength measurements. As a result, the average strength of the long fibers will be less than the strength measured using short fibers. Under static loading conditions this generally does not matter because the matrix provides load transfer between fibers thereby mitigating the effects of local weak spots.

The second major assumption that the chain-of-bundles strength models make is that the fibers are perfectly aligned and perfectly bonded to a flawless matrix. Or in other words, it assumes that the composite corresponds to the ideal composite model other than including fiber discontinuities. This assumption ignores the many small imperfections that are found in real composites such as matrix micro-voids and local fiber/matrix debonds or weaknesses. These small imperfections are key factors for tensile fatigue because they serve as damage initiation sites.

4.4 Analytical Model

4.4.1 Approach

The analytical model developed in this work is based on the three physical foundations described in the previous section that correspond to the three stages of fatigue life: initial damage or damage initiation, damage growth, and failure. As inputs, the model uses basic material properties combined with laminate quasi-static strength data but *does not* require any experimentally derived fatigue life data.

The overall approach of the fatigue life model developed in this work is summarized in **Error! Reference source not found.** The fatigue damage growth portion that forms the core of the model is based on a micromechanical fracture mechanics model for fiber-matrix interface damage growth. In general, however, it has been observed that the macroscopic behavior of a PMC cannot be accurately predicted using only micromechanical models. This is largely because the microstructure of real composites is too complex with far too many unknowns making it impossible to create micro-model accurate and complete enough to adequately predict the behavior of the whole composite (see discussion in section 4.3.1). To circumvent this problem, in this work the chain-of-bundles model is “calibrated” using quasi-static tensile strength data (which is experimentally much easier to obtain than fatigue life data). The result is a model that uses the real, as-manufactured properties of a particular material to provide a prediction of its tensile fatigue behavior.

The complete model can be divided into three primary component models: an initial damage model, a damage growth model, and a tensile failure model. These component models are described the following sections.

4.4.2 Initial Damage

A simple two-ply composite laminate consists of thousands of individual fibers. Consequently, measuring or modeling of every fiber at every point in a real composite is impossible, or at least unpractical. As a result a means to describe or characterize the initial state of the as-manufactured composite is required.

In the context of this discussion, *initial damage* refers to any free surfaces within the polymer matrix composite laminate that are present *after one initial load cycle*. These surfaces are created as a result of the natural flaws present in composite materials as discussed in section 4.3.1.

During the initial development of this model, the idealistic goal was to create a fatigue life model based entirely on the physical micro-scale mechanisms responsible for fatigue in a way analogous to fatigue crack growth models for metals. However, the problem of quantifying the initial damage (in a virgin material) quickly led to the conclusion that this is not feasible because it is unrealistic to gather enough data to model every fiber-matrix interface as is required by a pure micromechanics approach. The complexity and sample-to-sample variability inherent in polymer matrix composites led to the idea of using static tensile data as a key input to describe the initial damage state in a particular composite.

The mean value and distribution of the static tensile strength of the test laminate are the primary inputs to the model. Together they provide a measure of the initial internal damage state of the material, which is then used as a starting point for the damage growth model. A major benefit of using the tensile strength distribution for the whole composite (instead of just the *fiber* strength distribution) is that the effects of all other non-ideal aspects of the composite are accounted for.

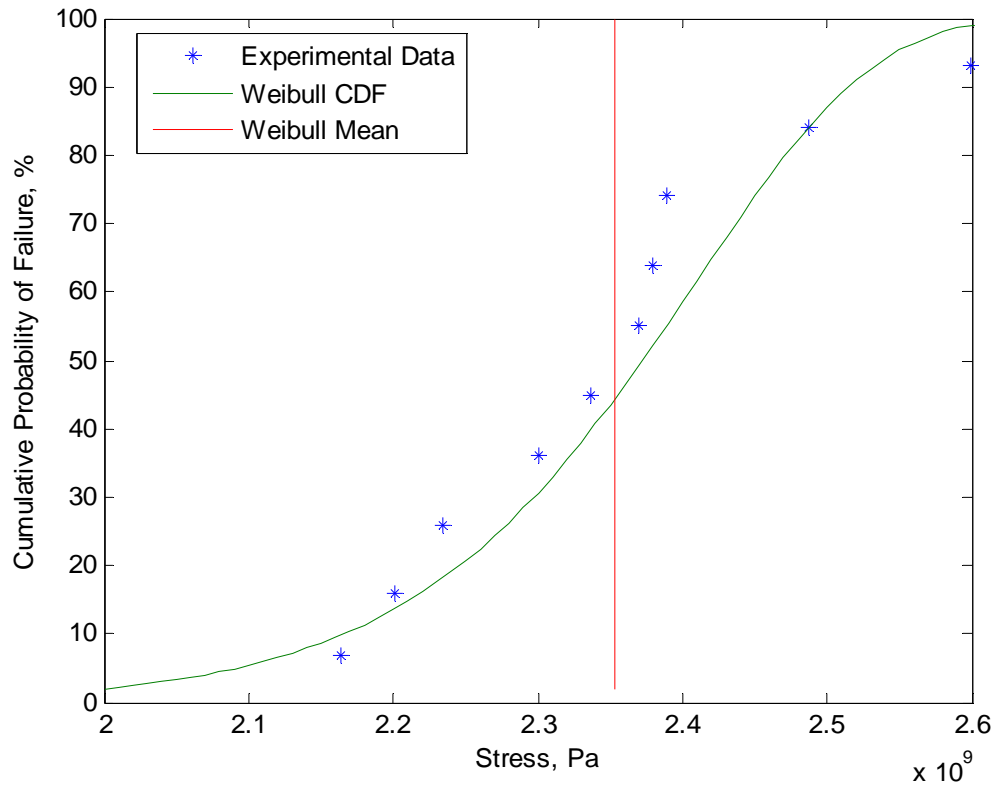


Figure 22: Cumulative distribution function and experimental data for quasi-static test specimens.

As discussed earlier, quasi-static tensile test data is the key input to the model because it is a measure of the initial damage state of the composite. The first step in using this model is to fit a two-parameter Weibull distribution to quasi-static tensile strength test data. There are several approaches to calculating the Weibull parameters, all of which are standard statistical analysis methods. In this work, the maximum-likelihood-estimation (MLE) method was used. Figure 22 shows the experimental data and the Weibull cumulative density function for the tests conducted in this work. This distribution gives a measure of the relative dispersion in the initial damage density.

The other key piece of information gleaned from quasi-static test data is a relative measure of the initial damage density. The initial damage fraction is calculated by comparison of the experimentally measured strength to the Rule-of-mixtures predicted strength as shown in Equation 19.

$$D_i = \left(X_{T,ROM} / X_{T,EXP} \right) - 1$$

Equation 19

Using the Weibull mean static strength and the distribution parameter α determined from quasi-static tensile testing, the distribution parameter for the apparent link strength, β_{Link} , is calculated using Equation 20. This equation is the result of the cumulative weakening strength theory described in section 2.2.2 rearranged so that the measured strength and the elastic ineffective length are used to solve for the distribution parameter, β . The result of this formulation is a measure of the link strength dispersion.

$$\beta_{Link} = \frac{\sigma_{Ult,Lam}^{-\beta}}{\alpha \delta_e e}$$

Equation 20

The elastic ineffective length, δ_e , is analytically calculated based on a simple shear-lag model and the properties of the fiber and matrix (Equation 21). This model is consistent with the chain-of-bundles models. The fiber stress recovery fraction, ϕ , is the fraction of the nominal fiber stress level below which a fiber is considered ineffective. This value was chosen to be 90% in this work to be consistent with the general chain-of-bundles models implemented in the literature.

$$\delta_e = \frac{d_f}{2} \left(\frac{1 - \sqrt{v_f} E_f}{\sqrt{v_f} G_m} \right) \cosh^{-1} \left(\frac{1 + (1 - \phi)^2}{2(1 - \phi)} \right)$$

Equation 21

By using the laminate tensile strength in addition to fiber and matrix properties, this method captures the actual characteristics of the composite, including all of the initial defects/flaws. As such, this method is superior to the traditional chain-of-bundles methods that use only the bare fiber strength distribution.

Next, the initial actual ineffective length for the composite is calculated using the apparent link strength distribution parameter, β_{Link} calculated in the previous step and the measured static strength. Again, since the value of the initial ineffective length is derived from experimental data it reflects the actual state of the real composite. Comparison of this value to the elastic ineffective length can be taken as a relative measure of the *initial damage state* for the composite.

$$\delta_i = \frac{\sigma_{Ult,Lam}^{-\beta_{Link}}}{\alpha \beta_{Link} e}$$

Equation 22

4.4.3 Damage Growth Threshold

In general, a composite will not suffer fatigue damage if the maximum cyclic load is below a certain fraction of the composites ultimate tensile strength. This is analogous to fatigue in metals where a crack will not grown unless the stress at the crack tip is above a critical value, such as K_{Ic} for Mode I crack growth. This critical value is a *material property* and does not depend on the structural geometry or load level.

Surprisingly, most tensile fatigue models for PMCs *do not* include a damage growth threshold for damage growth. This is likely due to the empirical foundation of most fatigue life analysis methods for composites and reflects the lack of fundamental understanding of the mechanisms that cause tension-tension fatigue damage and failure in PMCs.

A key consideration in the development of the damage growth model in this work was the inclusion of a damage growth threshold. A model that is truly based on the physical mechanisms responsible for fatigue a damage growth should naturally incorporate a damage growth threshold. In this work, the damage growth threshold is implemented by comparing the strain energy available in the fiber/matrix bond in the neighborhood of a fiber break/discontinuity to the critical strain energy release rate. Within the scope of this model (uniaxial tensile fatigue) only Mode II strain energy is considered and the damage grown threshold criteria is shown in Equation 23. (The calculation of the strain energy release rate is given in the next section, 4.4.4).

$$G_{Fiber/Matrix} \geq G_C \text{ or } G_{II} \geq G_{IIC}$$

Equation 23

4.4.4 *Damage Growth Model*

The fatigue effect in general refers to some type of damage that grows as a result of cyclic loading. For the case of fatigue of metals, the damage growth is one [critical] crack that grows (in a self-similar manner) in response to cyclic loading. In contrast, damage growth in composites is not due to one single crack, but the growth of many (thousands) of smaller cracks. As stated earlier, in composites the type of damage that both grows under cyclic

loading *and* directly affects the tensile strength of polymer matrix composites is fiber/matrix interface damage.

The damage growth model developed in this work uses fracture mechanics of the fiber/matrix interface to model the damage growth. The basis of the damage growth model is a model of the fiber/matrix interface failure (crack) that grows as a result of shear loading. In other words, the model is based on Mode II crack growth between the fiber and the matrix. Because only Mode II crack growth is considered, this model is restricted to uniaxial composites only. However, successful development and demonstration of this limited model is a necessary first step in the creation of a more comprehensive model.

The basic unit of the model is a single fiber/matrix model encompassing a fiber break and a fiber/matrix interface failure zone (Figure 23). This is an extension of the model presented in section 2.2.2 and shares all of the assumptions and restrictions of that model. As before, the model is centered about a fiber fracture over which no tensile load (stress) is supported. Additionally, the fiber is assumed to carry no load in the region surrounding the fracture where the fiber/matrix interface is failed.

During each loading cycle where the damage growth threshold is exceeded, the fiber/matrix interface crack will grow parallel to the fiber for a length da according to the crack growth law described in this section.

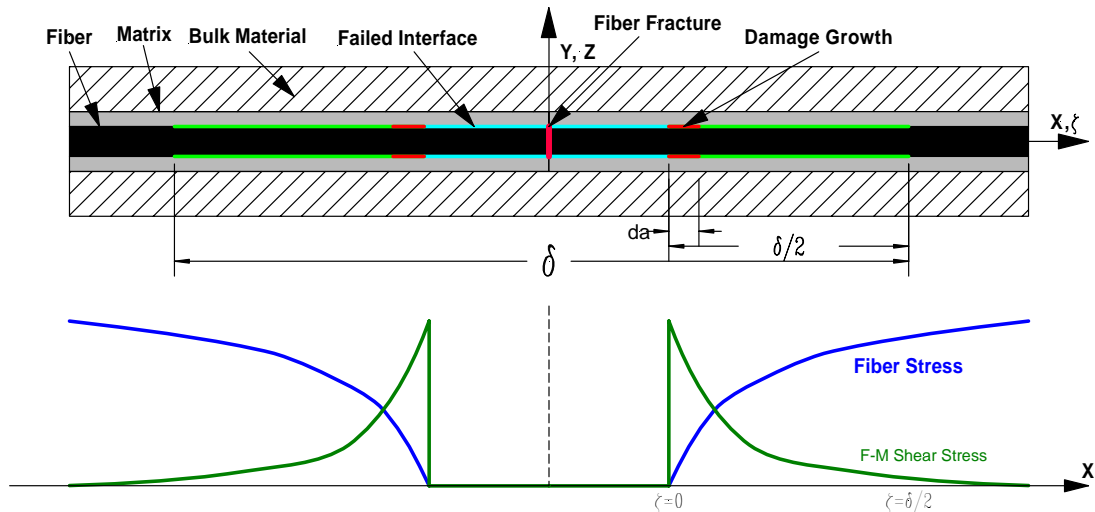


Figure 23: Fiber/matrix interface damage growth model

The fiber/matrix interface crack growth model is assumed to follow the traditional Paris-type crack growth equation,

$$\frac{da}{dN} = C\Delta G^m$$

Equation 24

where C and m are the crack growth constants. However, in pursuit of the goal of developing a model that does not explicitly require S-N data, in the model developed in this work the crack growth constant C was assumed to be inversely proportional to the nominal fiber stress level, and the crack growth constant m was taken as unity. These choices were made as logical first-cut estimates for model development and are a good subject for future research.

The strain energy release rate, ΔG , is calculated as the difference between the maximum shear strain energy in the fiber/matrix interface failure zone on one side of the fiber break and the critical shear strain energy release rate of the fiber/matrix interface.

Based on the assumption that progressive damage growth only occurs at the initial damage sites, the crack growth rate is multiplied by the initial damage fraction, D_i . The resulting fiber/matrix interface crack growth equation is given below as Equation 25.

$$\frac{da}{dN} = \frac{1}{\sigma_{f_0}} (G_{II} - G_{IIC}) D_i$$

Equation 25

The strain energy release rate, G , for the single fiber/matrix interface failure model is evaluated using traditional shear-lag analysis.

$$G = \frac{d\Pi}{dA} = \frac{dU}{dA}$$

Equation 26

The shear strain energy, dU , is calculated by integrating the shear force in the fiber/matrix interface on one side of the fiber break. Integration is taken over one half of the elastic ineffective length corresponding to the distance from where the fiber is broken or otherwise unloaded to where it is loaded to 90% of the nominal fiber stress.

$$dU = \int_{\zeta=0}^{\zeta=\delta_E/2} \tau A \gamma d\zeta = G \pi d_f \int_{\zeta=0}^{\zeta=\delta/2} \gamma^2 d\zeta$$

Equation 27

Using the shear lag model given in section 2.2.2 and carrying out the integration of Equation 27, the following expression for the strain energy in the fiber/matrix failure zone is obtained:

$$dU = \frac{1}{16} \pi d_f \sigma_{f_0}^2 \frac{v_f^{1/2}}{E_f (v_f^{1/2} - 1)} \frac{(2\eta\delta_E + e^{2\eta\delta_E} - 1)e^{-2\eta\delta_E} - 2}{\eta^2}$$

where:

$$\eta = 2 \sqrt{\frac{G_M \sqrt{v_f}}{E_f (1 - \sqrt{v_f}) d_f^2}}$$

Equation 28

Finally, the strain energy release rate is evaluated by normalizing the strain energy by the area of the fiber/matrix interface corresponding to the elastic ineffective length.

$$G_{II} = \frac{dU}{dA} = \frac{dU}{\delta_e \pi d_f}$$

Equation 29

This single fiber/matrix damage growth model is applied to the whole laminate by assuming that the greatest damage growth occurs at the critical initial damage site and that this damage is the limiting factor on the tensile strength. Recall that static tensile strength distribution used for defining the initial damage state is derived from static tensile strength data. In the static tensile data the strength is assumed to be limited by the strength of the weakest link in the laminate, which physically corresponds to the location having the greatest flaw density, or defined here as the critical initial damage state.

Furthermore, it is assumed that the properties of the fibers themselves do not degrade as a result of fatigue loading, and that critical fatigue damage *only* develops at the initial damage sites therefore the effects of any new damage sites generated after the first load cycle are negligible.

Recall that *initial damage* refers to fiber discontinuities, fractures, etc. that are present after one tension loading cycle. This accounts for the occurrence of fiber ends *and* fiber

fractures that develop during initial loading as a result of manufacturing defects, as shown in Figure 20.

4.4.5 Failure Model

The final part of the analytical fatigue life model is the tensile failure model. The objective of the failure model is to provide a means to predict when the composite will suffer catastrophic tensile failure as a result of the damage developed during cyclic tensile loading. An important requirement for the failure model is that it must consider [account for] the original distribution of static strength in addition to the effects of damage developed during cyclic loading.

The approach taken in this work is to start with the initial strength distribution and apply to it the effects of fatigue damage. This is implemented via two key ideas that are at the heart of this method. The first is that tensile failure (both static and fatigue) is a function of the ineffective length and can be predicted using a chain-of-bundles modeling approach. The second key idea is that fatigue damage results in growth of the total ineffective length. Both of these concepts have been previously discussed in this document and have been implemented in various forms by other researchers. The approach is summarized in Equation 30 where δ_i is the initial ineffective length (as calculated from static test data) and δ_n is the ineffective length growth due to fatigue induced fiber-matrix interface damage.

$$X_T(\delta) = X_T(\delta_i + \delta_n)$$

Equation 30

After the damage growth rate has been calculated, the cumulative damage length can be calculated. This is done by multiplying the damage growth rate (per cycle) by the total number of cycles. The ineffective length after fatigue cycling is then the sum of the initial ineffective length and the cumulative ineffective length growth due to cyclic loading. Note that the ineffective length growth is two times the crack length growth because both sides of the fiber break must be considered.

The model then simply consists of adding the fatigue induced fiber-matrix damage to the initial ineffective length (as determined from static tensile data) resulting in the total ineffective length after N loading cycles.

$$\delta_N = \delta_i + 2 \int_{n=1}^N \frac{da}{dn}$$

Equation 31

The most probable residual strength of the composite can then be calculated using the chain-of-bundles model and the new ineffective length, δ_N , as given in Equation 32. This result can then be used to generate an S-N curve of the most probable fatigue life as shown in Figure 24.

$$\sigma_N = (\alpha \beta \delta_N e)^{-1/\beta}$$

Equation 32

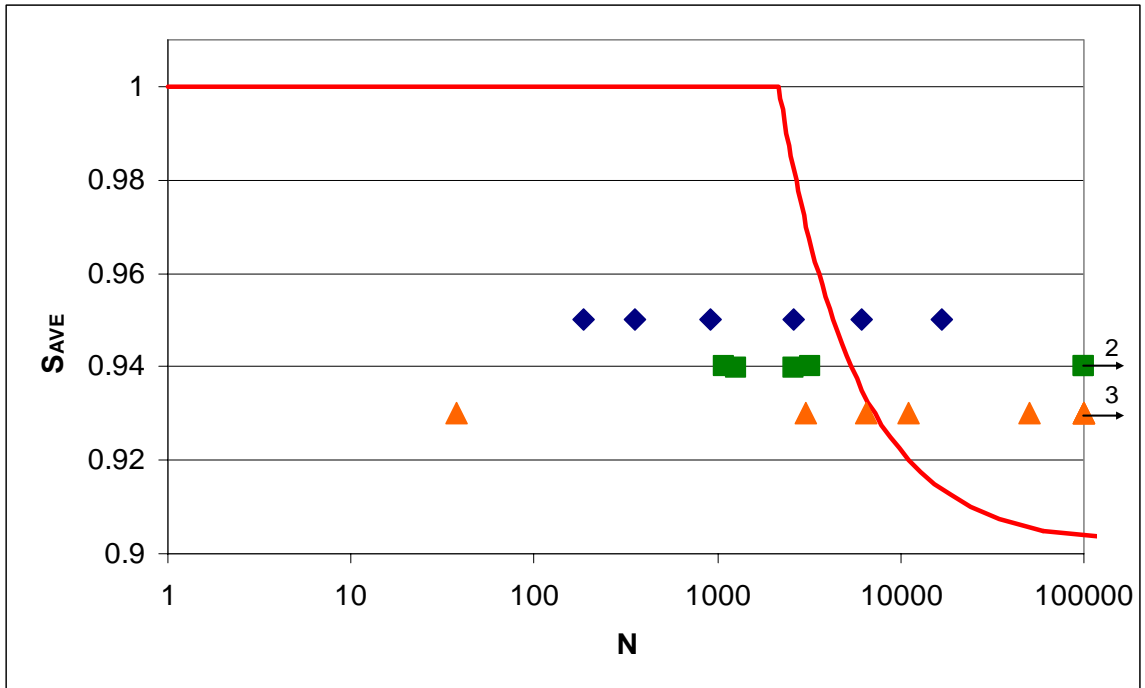


Figure 24: S-N curve calculated from Equation 32 using material properties of experimental test material.

4.4.6 Fatigue Life Distribution

Although a discrete S-N relationship is given by Equation 32, this single-value relationship for the fatigue life is not very useful because it does not account for the wide scatter in fatigue life that is characteristic of uniaxial composites as typified by the experimental results shown in Figure 24. This is because a discrete S-N relationship does not account for the natural variation in the microstructure of composites that gives rise to the non-deterministic nature of fatigue in PMCs. Instead of predicting single S-N points, it is much more useful to predict the *distribution* of fatigue life.

The first step in determining the fatigue life distribution is calculating the residual strength distribution after a series of particular S and N values. This is accomplished by using the

mean strength after cycling (σ_N , given by Equation 32) to calculate the new effective Weibull location distribution parameter, α_N for the material after a specific S-N history.

$$\alpha_N = \frac{\sigma_N^{-\beta}}{\delta_e \beta e}$$

Equation 33

Note that in this calculation, it is assumed that the distribution parameter, β , remains constant throughout fatigue cycling. This is a reflection of the assumption that damage growth occurs *only* at the location of the initial damage sites and that the fibers themselves do not degrade under fatigue loading.

The residual strength cumulative distribution function for a particular loading history can now be calculated using the new strength distribution location parameter, α_N , as shown in Equation 34. From this function the probability of fatigue failure can be directly obtained.

$$P(N|S, n) = 1 - \exp(-(\sigma \alpha_N)^\beta)$$

Equation 34

The result of this method is the residual strength distribution after fatigue cycling. Results for the test material used in the experimental portion of this study are given in Figure 25 for $S = 0.95$ and $N = 30,000$. Using the CDF curve the probability of failure can be readily calculated as the point where the peak applied load (S) equals the residual strength as shown in Figure 26.

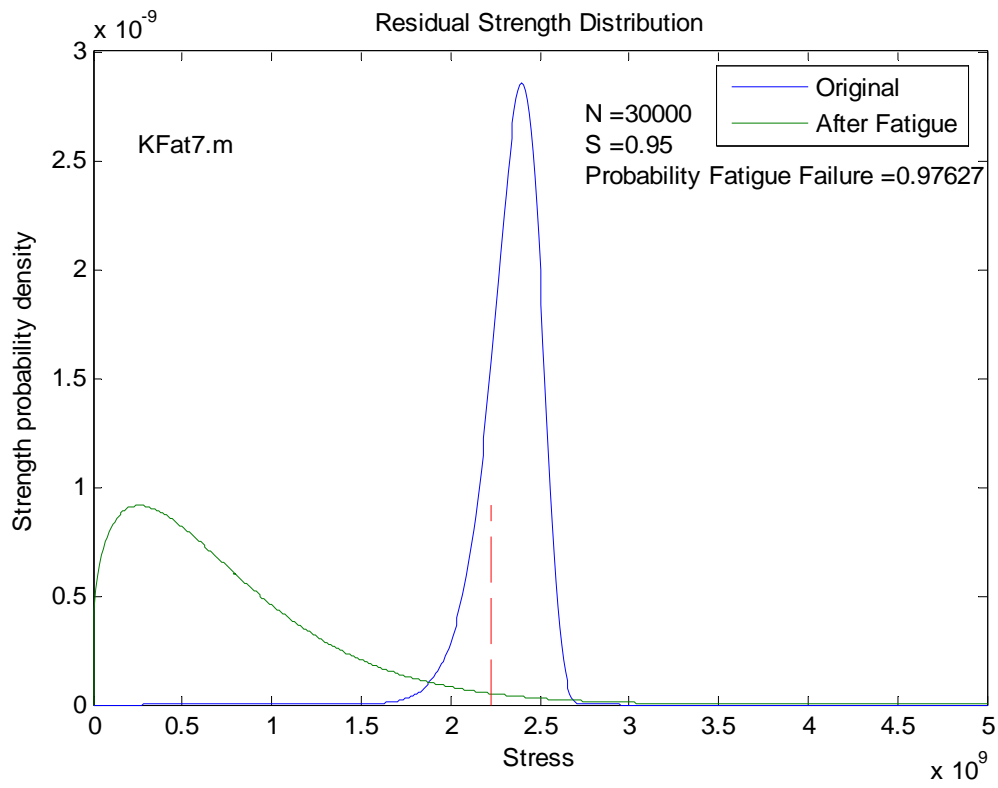


Figure 25: Tensile strength probability distribution for the test material before and after fatigue cycling at $S=0.95$ for 30,000 cycles (stress given in Pa).

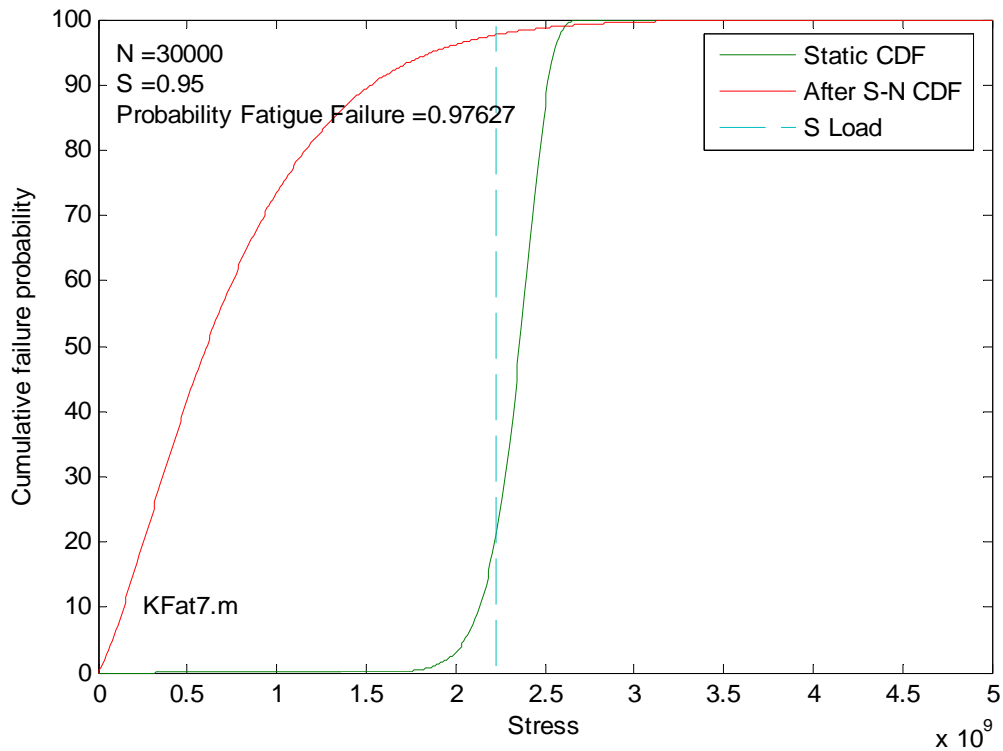


Figure 26: Cumulative probability of failure (percent) for the test material before and after 30,000 fatigue cycles at S=0.95 (ordinate axis units are Pa)

4.4.7 Fatigue Life CDF Bounds

The probability of fatigue failure is bounded by the probability of failure on the first load cycle and the probability of infinite life. The probability of failure on the first cycle is determined by comparison of the maximum applied stress to the static strength distribution. In other words it is the probability that the strength of a particular specimen is less than the maximum applied stress in the first load cycle.

On the other hand, the probability of infinite life is determined by the damage growth threshold and the static strength distribution. For a particular specimen, if the initial

damage density is small enough such that the maximum applied stress during loading does not result in local stresses exceeding the damage growth threshold for fiber/matrix interface damage then there will not be progressive damage growth therefore the specimen will have infinite life. This value is calculated as the probability that the static strength of the virgin laminate is such that the maximum applied cyclic stress (SX_{mean}) is less than the critical damage growth threshold stress level.

Using the upper and lower boundaries of the fatigue failure probability distribution, the fatigue failure distribution is obtained by linearly scaling the failure probability curve given by Equation 34 to fit between the upper and lower bounds. The result is a prediction of the cumulative probability of fatigue failure as a function of N for a given S load, including the probability of first cycle failure and the probability of infinite life, as shown in Figure 27. The upper limit of each curve is the maximum probability that a specimen will suffer fatigue failure, or one minus the probability that a particular specimen *will not* suffer critical fatigue damage growth and therefore exhibit infinite life. The lower limit is the probability that a specimen's strength is less than the maximum applied load and therefore it will fail on the first loading cycle.

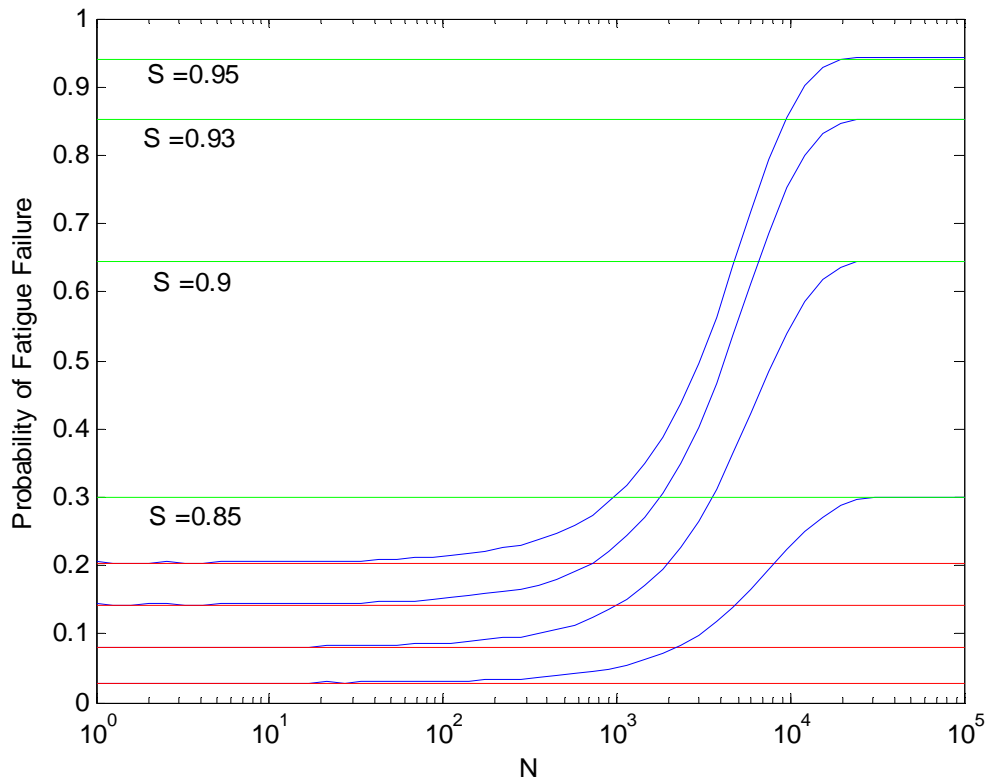


Figure 27: Example of the cumulative probability of fatigue failure predicted by the analytical model using the mechanical properties of the test material

4.5 Comparison of Experimental Data and Model Prediction

Although the limited number of samples at each S loading case makes the data set collected in this work not well suited for validation of the analytical model, several observations can be made that lend credence to the approach and the physical principles upon which the model is based. Specifically, the experimental data and the model results support the following conclusions:

- I.* The model independently validates the generally accepted fatigue failure domain diagram as originally presented by Talreja et al (see dissertation section 2.1.2:

Fatigue Damage Mechanisms in Unidirectional Composite Laminates). This framework states that the S-N fatigue failure behavior of unidirectional composites is comprised of three discrete domains corresponding to low, middle, and high cycle fatigue: failure due to random fiber fracture, failure due to weakening from progressive damage growth, and infinite life because critical damage does not develop. As illustrated by the predicted most probable S-N curve shown in Figure 24, the model developed in this work analytically predicts such behavior using only material mechanical properties and static test data [as inputs].

2. The model prediction and experimental results agree well with respect to the N range over which fatigue failure is likely to occur. The model developed in this work analytically predicts this range without using any fatigue life data for inputs. All experimental fatigue failures (with the exception of one point in the $S=0.93$ data series) occurred comfortably within the predicted range.
3. The model predicts the occurrence and frequency of runout tests, or tests in which critical damage is not developed as a result of cyclic loading for the given loading conditions. The model predictions and experimental results are given in Table 5. The low number of test points for each S load makes for a weak comparison, but the trend of the experimental results agrees with the model prediction.

Table 5: Occurrence of runout tests in experimental fatigue data

S	Predicted % Runouts	Experimental result
0.95	5%	0/6
0.94	10%	2/6 (33%)
0.93	15%	3/8 (38%)

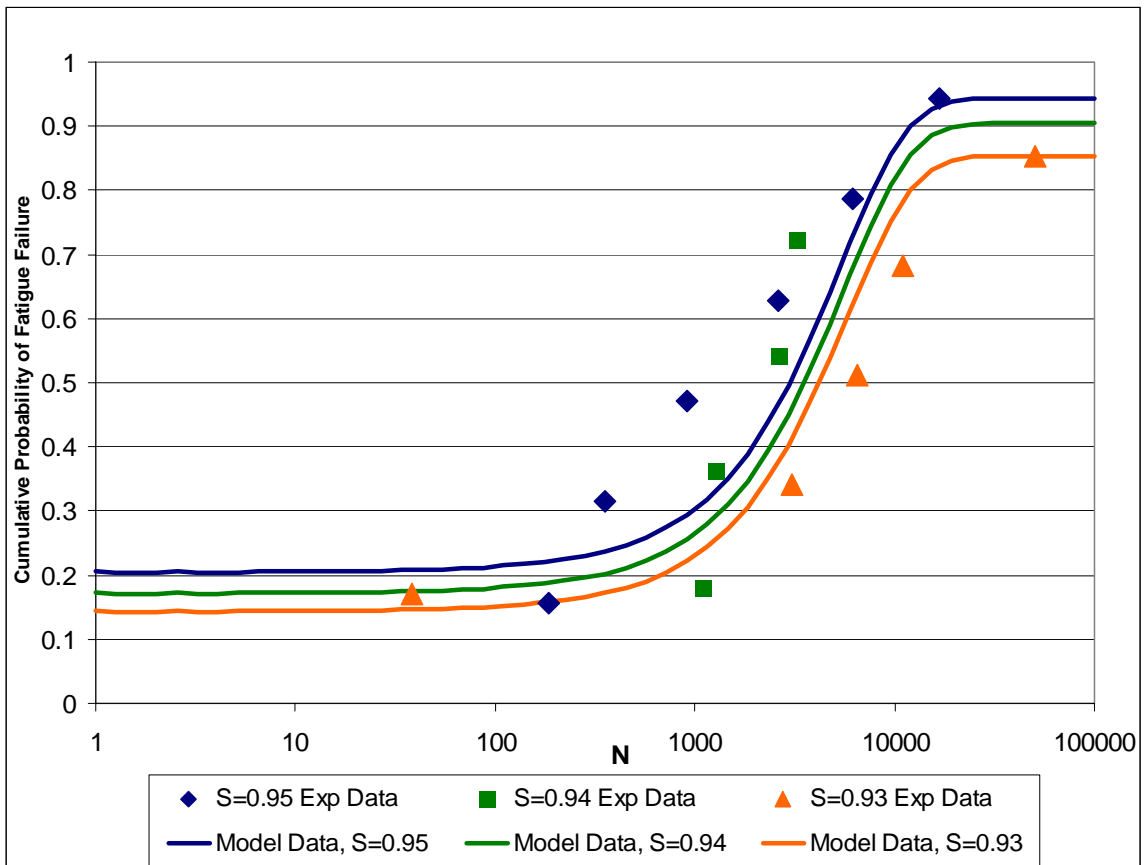


Figure 28: Experimental data distribution compared to predicted fatigue life distribution

In Figure 27 the experimental fatigue failures are plotted according to their normalized rank amongst the set of fatigue failures for each S load. The normalized rank for each fatigue failure is calculated by the rank of each sample within each S data series multiplied by the analytically predicted probability of infinite life for that S load (Equation 35). This

normalization method is necessary because the present experimental data set is far too small to provide a statistically significant value for the frequency of runout tests.

$$NormRank(i) = \frac{Rank(i)}{Total \# Fatigue Failures} P(N = \infty)$$

Equation 35: Calculation of the normalized rank of experimental data points for comparison to the analytical model prediction

4.6 Parameter Sensitivity

To help assess the validity of the model results, a brief parameter sensitivity study was conducted to determine the effects of hypothetical variations of the model inputs. The critical strain energy release rate was chosen as an ideal candidate for variation because its value can significantly differ between material systems. As shown in Figure 29, increasing this value causes the fatigue life prediction curve to skew to the right towards higher cycles. Physically, this is indicative of the damage growth rate being reduced as a result of a higher critical strain energy release rate and corresponds to qualitatively expected behavior.

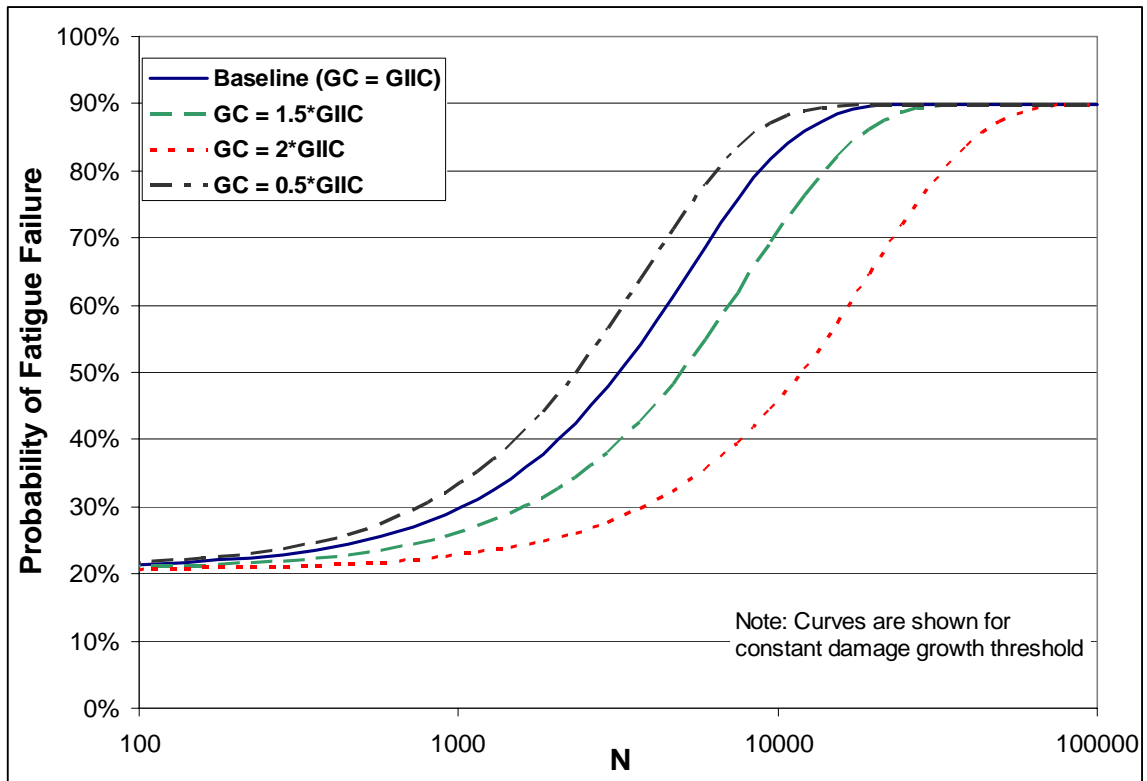


Figure 29: Effect of Strain Energy Release Rate Change on the predicted fatigue life distribution for $S=0.95$

4.7 Model Results

This section presents a discussion of the results and observations gleaned from the experimental data and the development of the analytical model.

Experimental Distribution

The experimental fatigue life data gathered in this study (shown in Figure 18) exhibits significant scatter. In fact, the scatter is so great that at first blush the data seems to exhibit no obvious consistent fatigue behavior. The scatter in this experimental data is consistent with other researchers' findings of uniaxial composite fatigue life tests where the lifetime

distribution is very wide and data sets often include instances of both run-out and instantaneous failure and has led some researchers to conclude that uniaxial composites do not exhibit consistent/true fatigue behavior. However, the model developed in this work predicts both a wide S-N distribution and runout/first cycle failure as natural artifacts of the fundamental nature of fatigue in uniaxial composites.

Fundamentally, the wide distribution of fatigue life data can be attributed to the fact that the true static strength of a particular specimen is not precisely known. Composites, especially uniaxial laminates, exhibit significant scatter in static tensile strength, with coefficients of variation typically ranging from 4% to upwards of 10% within a given population. As a consequence there is substantial uncertainty in the actual S load that is applied to a particular test specimen because the S load is (by necessity) defined as a fraction of the *mean* strength for the whole population. For any particular specimen [from that population] the *actual S load* may well be greater or less than the intended S load. As a result, the fatigue life of a population for a particular S load will take on a distribution that is a reflection of the population's static strength distribution.

Runout and First-Cycle failure

In addition to having a wide fatigue life distribution, the experimental data gathered in this work includes several instances of fatigue runout. Although at first blush this seems to indicate some sort of experimental inconsistency or error, the occurrence of these runout specimens actually fits well within the model framework. Again, because strength of a

particular material is not characterized by a single value but instead by a somewhat wide distribution, the actual S load on some specimens may be less than the damage growth threshold. The test material used in this study (IM7/8552) turns out to have a high damage growth threshold (for Mode II loading) relative to its static strength. As a result, for lower *mean* S loads (greater than but close to the damage growth threshold value) the *actual* S load applied to certain specimens was below the damage growth threshold. Consequently, these test specimens did not show progressive damage growth and therefore reached the runout cycle count without failing. Conversely, some specimens may have a higher than average initial damage density and therefore have lower than average strength. If the actual strength of a particular specimen is less than the maximum applied load (defined as $S\sigma_{ULT}$) then it will fail on the first load cycle. This idea is illustrated in Figure 30 which shows the static strength distribution from the tests in this work along with the maximum applied stress for $S = 0.95$ and the damage growth threshold stress level.

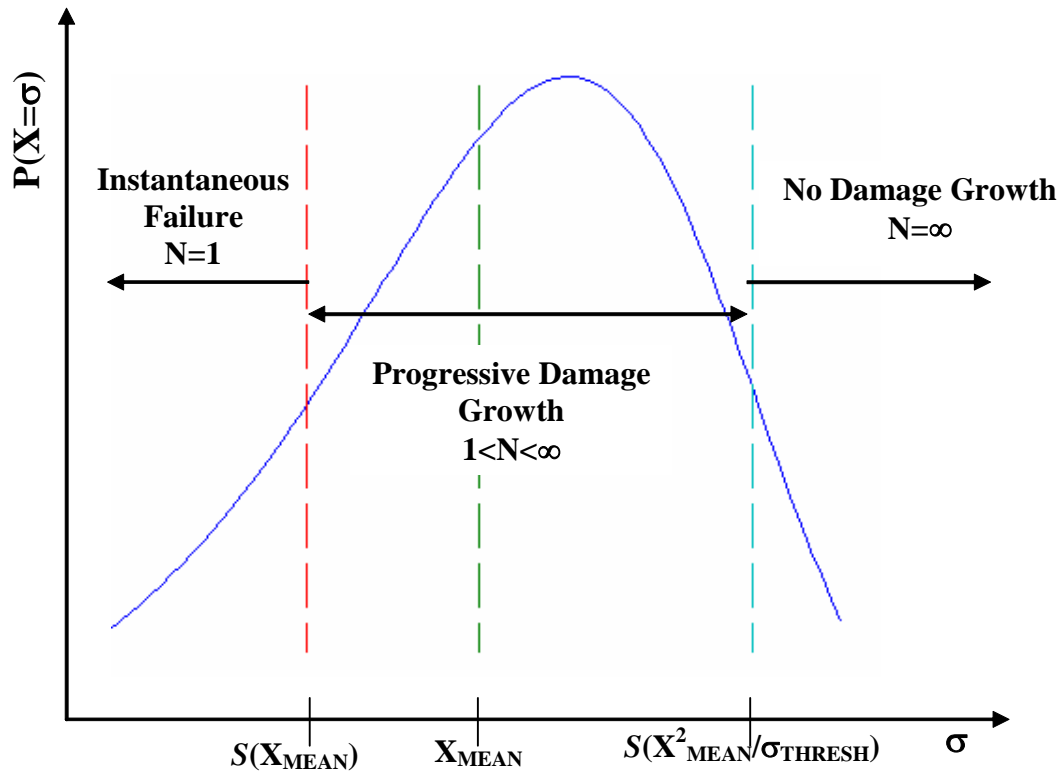


Figure 30: Static strength distribution for the test material showing damage growth threshold and peak applied stress for $S=0.95$.

One of the greatest drawbacks of current deterministic fatigue life prediction methods is that they cannot easily account for the inherent variability and uncertainty in the tensile strength of composites. Alternatively however, probabilistic methods are readily adapted to the problem. For example, by using the strength distribution of the test laminate as an input, the method developed in this work captures the actual material characteristics of a particular experimental population. The result of the model is then the probability of failure at some S-N point rather than specifying failure at a single S-N point. Additionally, the probability of a particular specimen reaching the runout criteria or failing on the first load cycle is also calculated. In summary, the approach used in this model addresses the

uncertainties associated with composites and their impact on the materials tensile fatigue response.

CHAPTER 5: SUMMARY AND CONCLUSIONS

5.1 Summary of Key Concepts

The fatigue model developed in this work adds new support to the idea that fiber-matrix interface damage is the primary mechanism responsible for fatigue in uniaxial composites. Additionally, the implementation and demonstration of a non-deterministic approach to fatigue life analysis (of uniaxial PMCs) leads to some important observations relevant to the fatigue behavior of uniaxial composites. This section presents a summary of the key ideas and observations developed in this work.

The key idea that forms the foundation of this model is that *fiber-matrix interface damage is the dominant physical mechanism responsible for tensile strength degradation and failure in uniaxial composites under tensile fatigue loading*. Although in itself this is not a new idea, the results from the analytical model developed in this work add strong new evidence to support this conclusion. Specifically, because this model does not use any S-N data for fitting the model to the experimental data but instead uses a fracture mechanics approach to describe fiber-matrix interface damage growth, it gives strong support to the conclusion that fiber-matrix interface damage is the key mechanism responsible for fatigue in uniaxial polymer matrix composites.

The central idea in the damage growth model developed in this work is that *fiber-matrix interface damage can be modeled using traditional fracture mechanics techniques*. These techniques allow straightforward calculation of damage growth and easy implementation of

a damage growth threshold. Again, because the model developed here does not use S-N fitting data it demonstrates that approaches using fracture mechanics for damage growth modeling are viable. The damage growth model used in this work is very simple and limited, but it provides a good demonstration of the potential of such methods.

To implement the micromechanical damage growth model, data about the initial damage state of the laminate is required. A key aspect in the development of this model is understanding and accounting for the non-ideal microstructure of real composites. By necessity, pure micromechanics-based performance models must assume that the physical layout of the composite follows some type of known and predictable pattern—for example that all fibers are parallel and perfectly bonded to the matrix. In reality however, that is simply not true, as discussed in section 4.3.1. Recognizing that it is impossible (or at best extremely impractical) to thoroughly inspect and gather data about the precise microstructure of every point in a composite, the method developed in this model makes use of tensile strength data combined with basic mechanical properties to quantify the initial damage state of a real, as-manufactured laminate.

The micromechanical damage growth model is applied to the macromechanical behavior of the real (non-ideal) composite using a chain-of-bundles type model. These types of models have previously been used in a variety of different projects because they enable macroscopic laminate behavior, generally tensile strength, to be predicted using the microscopic properties of the constituent materials and the laminate microstructure. However, the major flaws with these approaches are that they require accurate knowledge

of the bare-fiber strength statistics and they assume the composite has an ideal microstructure. As previously discussed, the latter assumption is not valid for real composites and bare fiber strength statistics are not commonly or easily obtained.

To circumvent these problems, the method developed in this work uses the observed macromechanical material properties (tensile strength data) as the primary input instead of micromechanical data. This is accomplished by essentially employing the chain-of-bundles model in reverse—using laminate static tensile strength data and basic constituent properties to calculate the effective micromechanical characteristics of the material (namely the initial ineffective length, the critical ineffective length, and the link strength distribution). Because assumptions about the composite microstructure are necessary to do this, the calculated micromechanical properties are not necessarily representative of the true physical system. However, since the objective is not to determine the micromechanical characteristics but instead to obtain data to enable the application of a damage growth model this pseudo-physical representation is acceptable. In essence, the chain-of-bundles model serves as a bridge between the macroscopic and microscopic aspects of composite laminate behavior.

5.2 Summary of Results

A model for predicting the fatigue response of uniaxial composite laminates under tension-tension fatigue loading was developed. This model is based on three physical

foundations/principles that were identified as characterizing the tensile fatigue process in uniaxial composites. These are:

1. The *initial damage* in a virgin composite laminate is due to the non-ideal aspects of a composites microstructure. This initial damage is present in all composites due to the inherent variability and complexity of these multi-phase materials.
2. The type of damage that grows as a result of tensile fatigue loading and directly affects the ultimate tensile strength is *fiber-matrix interface* damage. This progressive damage can be modeled using traditional fracture mechanics techniques.
3. The tensile strength of a uniaxial composite is dependent on the integrity of the fiber-matrix interface. Fatigue loading can damage the fiber-matrix interface thereby reducing the ultimate tensile strength of the composite. Tensile failure then occurs when the composites strength is reduced to equal the applied load.

The model (summarized in

Figure 31) uses static tensile strength data and basic material properties to calculate the strength degradation due to fiber-matrix damage growth caused by fatigue loading. The output of the model is the strength distribution after a specified number of load cycles from which the probability of fatigue failure can be directly calculated.

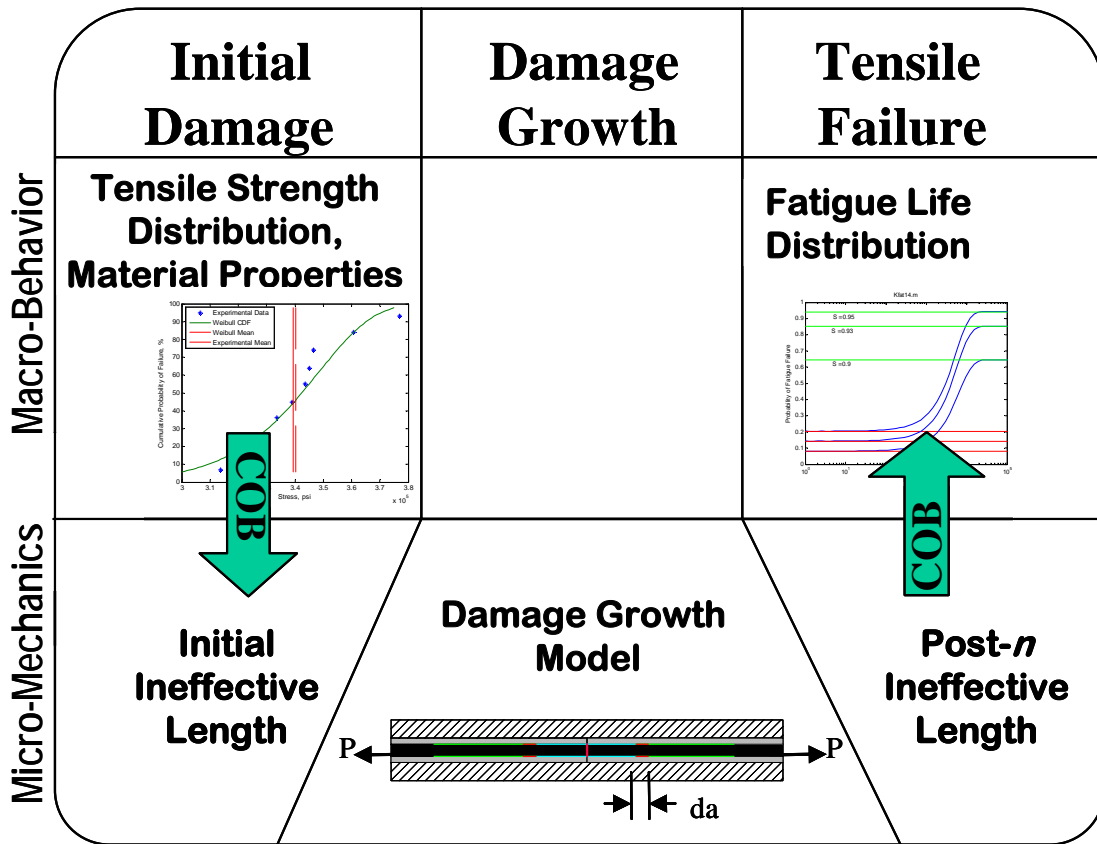


Figure 31: Functional summary of the fatigue life model developed in this work.

An experimental test program was conducted as part of this work in order to provide data for comparison to and verification of the fatigue life model. The results of the uniaxial tension-tension fatigue testing are consistent with data in the literature and yield the following key observations.

1. The un-notched uniaxial polymer matrix composite test specimens exhibit a wide fatigue life distribution. For example, for an average peak cyclic load of $S=0.95$, the shortest fatigue life recorded was 185 cycles while the longest was 16,781 cycles.

2. The material tested (IM7/8552) has a high fatigue damage growth threshold for uniaxial tension tension fatigue corresponding to approximately 90% of the mean static tensile strength. Consequently, several of the test specimens did not fail and the fatigue tests were stopped when the runout criteria was met.

5.3 Conclusions

Several important conclusions have been gleaned through this work. These are:

- Deterministic fatigue life prediction models are not adequate for real composites due to the large number of unknowns in real composite materials.
- Non-deterministic analysis of the fatigue life of uniaxial laminates explains many of the statistical variations observed from experimental testing.
- The chain-of-bundles model for uniaxial composites can be used as a bridge enabling micro-mechanical damage growth models to be applied to determine the macro-mechanical behavior of real composites.
- Fiber-matrix interface damage can be modeled using traditional fracture mechanics techniques.

Throughout this work it has become increasingly evident that deterministic methods are not appropriate for fatigue life analysis of uniaxial composites because of the large number of unknowns in real composites. The microstructure of real composites is generally significantly different from and more complex than represented by the ideal micro-

mechanical model, and these variations *are the physical root causes* of fatigue damage growth and failure. Furthermore, the precise microstructure of composites, which constitutes the physical data needed for accurate deterministic models, is impossible to obtain in practical applications. The result of these unknowns is that deterministic fatigue life models suffer from the “garbage in- garbage out syndrome” and neither consider nor provide enough data to constitute a complete picture of uniaxial tensile fatigue.

Due to the complexity of damage growth and failure of unidirectional fiber reinforced composites, deterministic calculation of the fatigue life is not a very useful or reliable method and it is front-loaded with significant uncertainties. Instead, calculation of the *probability* of failure for a particular S-N value (or S-loading) provides a much greater depth of information and insight into the fatigue behavior. On the other hand, one of the biggest drawbacks of traditional non-deterministic methods is that they require even more data than deterministic methods! Consequently, it is not feasible to generate useful fatigue life prediction methods using only pure non-deterministic methods.

The method developed in this work successfully demonstrates an approach to reconcile the limitations and benefits of both deterministic and non-deterministic fatigue life prediction methods. This is accomplished by utilizing various techniques to create a model that is a hybrid of experimental data, non-deterministic analysis, and micromechanics. This unique combination is enabled by using the chain-of-bundles model as a bridge relating the micromechanical fiber-matrix scale analyses to the macromechanical behavior of real composites. The distinguishing aspect of this approach however is that the primary input is

the static tensile strength of the *finished laminate* instead of fiber and matrix properties. Not only is the static tensile data much more readily obtained (than bare fiber data), but more importantly, because it is a direct measurement of the state of the as-manufactured material it automatically accounts for microstructural variations and defects in the real composite.

5.4 Recommendations for Further Work

The model developed in this work lays the foundation for a new breed of fatigue life models for polymer matrix composites. As this model is applicable only to uniaxial stress states (where the fiber-matrix loading is solely Mode II), the obvious next step is to integrate Mode I loading into the damage growth model thereby enabling its application to multi-axial stress states.

APPENDIX A. REFERENCES

1. Attia, O.; Kinloch, A.J.; Matthews, F.L., "Modelling the fatigue life of polymer-matrix fibre-composite components," *Composites Science and Technology*, Vol. 61 N 15, pp. 2273-2283
2. Beaumont, P.W.R., Schultz, J.m., "Failure Analysis of Composite Materials," *Deleware Composites Design Encyclopedia*, Vol.4, L.A. Carlsson and J.W. Gillespie, eds., Technomic Publishing Co., 1990
3. Beyerlein, I. J., and Landis, C. M., "Shear-lag model for failure simulations of unidirectional fiber composites including matrix stiffness," *Mechanics of Materials* 31 (1999) 331-350
4. Broutman, L.J., Sahu, S., "A New Theory To Predict Cumulative Fatigue Damage in Fiberglass Reinforced Plastics", *Proceedings of the 2nd Conference on Composite Materials: Testing and Design*, ASTM STP 497, 1972, pp.170-188
5. Case, S. W., and Reifsnider, K. L., "MRLife11™, A Strength and Life Prediction Code for Laminated Composite Materials," Materials Response Group, Virginia Polytechnic Institute and State University, Blacksburg, Virginia 24061, August 28, 1998
6. Charewicz, A., and Daniel, I.M., "Damage Mechanics and Accumulation in Graphite/Epoxy Laminates," *Composite Materials: Fatigue and Fracture*, ASTM STP 907, H.T. Hahn, Ed., American Society for Testing and Materials, Philadelphia, 1986, pp. 274-297
7. Chen, A.S., Almond, D.P, and Harris, B., "In situ monitoring in real time of fatigue-induced damage growth in composite materials by acoustography," *Composites Science and Technology* 61 (2001) 2437-2443
8. Chen, P., Shen, Z., Yang Wang, J., "Prediction of the strength of notched fiber-dominated composite laminates," *Composites Science and Technology* 61 (2001) 1311-1321
9. Dharan, C.K.H., "Fatigue Failure Mechanisms in a Unidirectionally Reinforced Composite Material", *Fatigue of Composite Materials*, ASTM STP 569, American Society for Testing and Materials, 1975, pp. 171-188
10. Gouda, M., Prewo, K.M., McEvily, A.J., "Mechanism of Fatigue in Boron-Aluminum Composites," *Fatigue of Fibrous Composite Materials*, ASTM STP 723, American Society for Testing and Materials, 1981, pp.101-115
11. Halverson, H. G., Curtin, W. A., and Reifsnider, K. L., "Fatigue Life of individual composite specimens based on intrinsic fatigue behavior," *Int. Journal of Fatigue*, Vol. 19., No. 5., pp. 369-377, C.1997 Elsevier Science Ltd.

12. Hashin, Z., Rotem, A., "A Cumulative Damage Theory of Fatigue Failure", *Journal of Material Science and Engineering*, Vol.34, 1978, pp. 147-160
13. Hwang, W., and Han, K. S., "Fatigue of Composite Materials- Damage Model and Life Prediction," *Composite Materials: Fatigue and Fracture, Second Volume*, ASTM STP 1012, Paul A. Lagace, Ed., American Society for Testing and Materials, Philadelphia, 1989, 87-102
14. Jamison, R.D., "On The Interrelationship Between Fiber Fracture and Ply Cracking in Graphite/Epoxy Laminates," *Composite Materials: Fatigue and Fracture*, ASTM STP 907, H.T. Hahn, Ed., American Society for Testing and Materials, Philadelphia, 1986, pp. 252-273
15. Jamison, R. D., Schulte, K., Reifsnider, K. L., Stinchcomb, W. W., "Characterization and Analysis of Damage Mechanisms in Tension-Tension Fatigue of Graphite/Epoxy Laminates," *Effects of Defects in Composite Materials*, ASTM STP 836, American Society for Testing and Materials, 1984, pp.21-55
16. Johnson, E. P., "Composite Strength Statistics from Fiber Strength Statistics," MS Thesis, Naval Postgraduate School, 1991
17. Kasen, M.B., Schramm, R.E., Read, D.T., "Fatigue of Composites at Cryogenic Temperatures," *Fatigue of Filamentary Composite Materials*, ASTM STP 636 K.L. Reifsnider and K.N. Lauraitis, Eds., American Society for testing and Materials, 1977, pp. 141-151
18. Kumar, R., and Talreja, R., "Fatigue Damage Evolution in Woven Fabric Composites," 41st AIAA/ASME/ASCE/ASC Structures, Structural Dynamics, and Materials Conference and Exhibit Atlanta, GA, April 2000
19. Lebon, B., Baxevanakis, C., Jeulin, D., and Renard, J., "Fracture Statistics of a Composite Laminate," *Composites Science and Technology* 58 (1998) 765-771
20. Lee, J., Daniel, I. M., and Yaniv, G., "Fatigue Life Prediction of Cross-Ply Composite Laminates," *Composite Materials: Fatigue and Fracture, Second Volume*, ASTM STP 1012, Paul A. Lagace, Ed., American Society for Testing and Materials, Philadelphia, 1989, 19-28
21. Lifshitz, J.M., and Rotem, A., "An Observation on the Strength of Unidirectional Fibrous Composites," *J. Composite Materials*, Vol. 4 (January 1970), p. 133
22. Lorenzo, L., Hahn, H.T., "Fatigue Failure Mechanisms in Unidirectional Composites", *Composite Materials: Fatigue and Fracture*, ASTM STP 907, H.T. Hahn Ed., American Society for Testing and Materials, Philadelphia, PA 1986, pp.210-232

23. Mahiou, H., and Beakou, A., "Local Stress Concentration And The Prediction of Tensile Failure In Unidirectional Composites," *Composites Science and Technology Elsevier Science Ltd.* Vol. 57 (1997), pp. 1661-1672
24. Mao, H., and Mahadevan, S., "Probabilistic Analysis of Creep-Fatigue failure," 41st AIAA/ASME/ASCE/ASC Structures, Structural Dynamics, and Materials Conference Atlanta, GA, April 2002
25. McLaughlin, P. VD, Jr., "Life And Residual Strength of Unidirectional Fiber Composites," *Durability of Composite Materials, Proceedings of the 1994 Internation Engineering Congress and Exposition ASME, New York, NY, 1994,* pp. 59-73
26. Minnetyan, L., Chamis, C.C., "Cyclic Fatigue Degredation response Of Composite Structures," SAMPE ISSE, May 2002
27. Minnetyan, L., and Chamis, C. C., "Computational Simulation of Composite Fatigue Life," 41st AIAA/ASME/ASCE/ASH/ASC Structures, Structural Dynamics, and Materials Conference and Exhibition Atlanta, GA, April 2000, AIAA-2000-1759
28. Miyano, Y., and Masayuki, N., and McMurray, M. K., and Muki, R., "Prediction of Flexural Fatigue Strength of CRFP Composites Under Arbitry Frequency, Stress Ratio, and Temperature," *Journal of Composite materials,* Vol. 31, No. 6, pp. 619-638
29. Morris, E.E., "Filament Wound Composite Thermal Isolator Structures for Cryogenic Dewars and Instruments," *Composites for Extreme Environments,* ASTM STP 768 N.R. Adsit, Ed., American Society for Testing and Materials, 1982, pp. 95-109
30. National Materials Advisory Board, "Life Prediction methodologies for Composite Materials," Report on the Committee on Life Prediction Methodologies for Composite Materials National materials Advisory Board, Commission on Engineering and Technical Systems, National research Council, NMAB-60, 1991
31. Nettles, A. T., and Biss, E. J., "Low Temperature Mechanical Testing of Carbon-Fiber/Epoxy Resin Composite Materials," NASA Technical Paper 3663
32. Okabe, T., Takeda, N., Kamoshida, Y., Shimizu, M., and Curtin, W.A., "A 3D shear-lag model considering micro-damage and statistical strength prediction of unidirectional fiber-reinforced composites," *Composites Science and Technology* 61 (2001) 1773-1787
33. Reifsnider, K. L, "Durability and Damage Tolderance: Testing, Simulation, and Other Virtual Realities," *Composite Materials: Testing and Design. Thirteenth*

Volume, ASTM STP 1242, S.J. Hooper, Ed., American Society for Testing and Materials, 1997, pp. 45-59

34. Reifsnider, K. L., "Damage and Damage Mechanics," *Fatigue of Composite Materials*, K.L. reifsnider Ed., Elsevier Science Publishers B.V., 1990, pp. 11-77
35. Reifsnider, K. L., "Introduction (to book)," *Fatigue of Composite Materials*, K.L. reifsnider Ed., Elsevier Science Publishers B.V., 1990, pp. 1-9
36. Reifsnider, K.L., Stinchcomb, W.W., "A Critical Element Model of the Residual Strength and Life of Fatigue-Loaded Composite Coupons," *Composite Materials: Fatigue and Fracture*, ASTM STP 907, H.T. Hahn Ed., 1986, pp. 233-251
37. Rosen, B.W., "Tensile Failure of Fibrous Composites," *AIAA Journal*, Vol. 2., No. 11, November 1964, pp. 1985-1991
38. Rusk, D. T., Lin, K. Y., Swartz, D. D., Ridgeway, G. K., "Bayesian Updating of Damage Size Probabilities for Aircraft Structural Life-Cycle Management," *AIAA Journal Of Aircraft*, Vol. 39, No. 4, July-August 2002, pp.689-696
39. Schaff, J.R. and Davidson, B.D, "A Strength-Based Wearout Model for Predicting the Life of Composite Structures," *Composite Materials: Fatigue and Fracture (Sixth Volume)*, ASTM STP 1285
40. Schaff, J. R., Davidson, B. D., "Life Prediction For Composite Laminates Subjected To Spectrum Loading," *Durability of Composite Materials*, MD-Vol. 51 ASME 1994
41. Schon, J., "Model for predicting the load ratio for the shortest fatigue life," *Composites Science and Technology* 61 (2001) 1143-1149
42. Schutz, D., Gerharz, J.J., Alschweig, E., "Fatigue Properties of Unnotched, Notched, and Jointed Specimens of a Graphite/Epoxy Composite," *Fatigue of Fibrous Composite Materials*, ASTM STP 723, American Society for Testing and Materials, 1981, pp. 31-47
43. Sendeckyj, G.P., Stalnaker, H.D., Kleismit, R.A., "Effect of Temperature on Fatigue Response of Surface-Notched [(0/+45/0)S]₃ Graphite/Epoxy Laminate," *Fatigue of Filamentary Composite Materials* ASTM STP 636, K.L. Reifsnider and K.N. Lauraitis, Eds., American Society for Testing and Materials, 1977, pp. 123-140
44. Sendeckyj, G. P., "Life Prediction for Resin-Matrix Composite Materials," *Fatigue of Composite Materials*, K.L. reifsnider Ed., Elsevier Science Publishers B.V., 1990, pp. 431-483

45. Shankar, G., and Sundaresan, M. J., "Tensile Strength of Unidirectional Composites with Matrix Plasticity and Fiber/Matrix Debonding," MD-Vol. 48, Composites: Design and Manufacture for Cost Effectiveness, ASME 1994
46. Soden, P.D., Hinton, M.J., and Kaddour, A.S., "A comparison of the predictive capabilities of current failure theories for composite laminates," *Composites Science and Technology* 58 (1998) 1225-1254
47. Spearing, M., Beaumont, P.W.R.; Ashby, M. F., "Fatigue damage mechanics of notched graphite-epoxy laminates," *ASTM Third symposium on composite materials: Fracture and Fatigue*, ASTM STP 1110
48. Stinchcomb, W.W., Reifsnider, K.L., Yeung, P., and Masters, J., "Effect of Ply Constraint on Fatigue Damage Development in Composite Material Laminates," *Fatigue of Fibrous Composite Materials*, ASTM STP 723, American Society for Testing and Materials, 1981, pp. 64-84
49. Subramanian, S., Reifsnider, K.L., Stinchcomb, W.W., "A Cumulative Damage Model To Predict The Fatigue Life of Composite Laminates Including The Effect of a Fiber-Matrix interphase," *Int. Journal of Fatigue*, Vol. 17, No. 5, pp. 343-351, C.1995 Elsevier Science Ltd.
50. Talreja, R., "Estimation of Weibull Parameters for Composite Material Strength and Fatigue Life Data," *Fatigue of Fibrous Composite Materials*, ASTM STP 723, American Society for Testing and Materials, 1981, pp. 291-311
51. Talreja, R., *Fatigue of Composite Materials*, Technomic Inc., 1987
52. Talreja, R., "Statistical Considerations," *Fatigue of Composite Materials*, K.L. reifsnider Ed., Elsevier Science Publishers B.V., 1990, pp. 485-501
53. Turcic, B., "'Natural" phenomenological fatigue damage cumulation model for composite laminates," *Materials Science & Engineering A: Structural Materials: Properties, Microstructure and processing*, Vol. A130, No. 1, pp. 21-27
54. Wang, A.S.D., Chou, P.C., Alper, J., "Effects of Proof Test in the Strength and Fatigue Life of a Unidirectional Composite," *Fatigue of Fibrous Composite Materials*, ASTM STP 723, American Society for Testing and Materials, 1981, pp.101-115
55. Whitcomb, J.D., "Experimental and Analytical Study of Fatigue Damage in Notched Graphite/Epoxy Laminates," *Fatigue of Fibrous Composite Materials*, ASTM STP 723, American Society for Testing and Materials, 1981, pp. 48-63
56. Whitney, J.M., "Fatigue Characterization of Composite Materials," *Fatigue of Fibrous Composite Materials*, ASTM STP 723, American Society for Testing and Materials, 1981, pp. 101-11